EurJOC European Journal of Organic Chemistry

FULL PAPER

DOI: 10.1002/ejoc.201200946

Chlorinated BODIPYs: Surprisingly Efficient and Highly Photostable Laser Dyes

Gonzalo Duran-Sampedro,[a] Antonia R. Agarrabeitia,[b] Inmaculada Garcia-Moreno,*[a] Angel Costela,[a] Jorge Bañuelos,[c] Teresa Arbeloa,[c] Iñigo López Arbeloa,[c] Jose Luis Chiara,*[d] and María J. Ortiz*[b]

Keywords: Dyes/Pigments / Laser dyes / Photophysics / Fluorescence / Halogenation

A series of mono- to hexachlorinated BODIPY dyes have been prepared in good to excellent yields through the use of *N*-chlorosuccinimide as an inexpensive halogenating reagent. This library of chlorinated dyes allowed analysis in detail, from the experimental and theoretical points of view, of the dependency of the photophysical and optical properties of the dyes on the number and positions of the chlorine substituents on their BODIPY cores. Quantum mechanical calculations predict the regioselectivity of the halogenation reaction and explain why some positions are less prone to chlorination. The new chlorinated BODIPYs exhibit enhanced laser action with respect to their non-halogenated analogues, both in liquid solution and in the solid phase. In addition, chlorination is a facile and essentially costless protocol for overcoming important shortcomings exhibited by commercially available BODIPYs, which should favor their practical applications in optical and sensing fields.

Introduction

In the past year alone, over 500 articles have been published on the synthesis and applications of 4-bora-3a,4a-diaza-*s*-indacene dyes, known as BODIPYs. The growing interest in these versatile fluorophores is due to their favorable spectroscopic properties, characterized by high absorption coefficients, high fluorescence quantum yields, high photostabilities, and low sensitivities to medium effects.[1] Currently, the development of new BODIPY dyes is driven by their potential applications as sensors in biology and in clinical diagnosis,[1g,2] as photosensitizers for photodynamic therapy (PDT),[3] and as laser generators,[1f,4] as well as for the manufacture of waveguides,[5] light-emitting diodes (OLEDs),[6] photovoltaic cells,[7] and electroluminescent devices,[6] in addition to the usual conventional applications of organic dyes. These and other emerging uses are conditioned by the emission wavelength, quantum yield, and stability of a given dye under the working conditions needed for each specific application; these can be particularly demanding, as is often the case with the new imaging techniques developed in optical microscopy that demand high-intensity laser irradiation.

The photophysical properties of a BODIPY dye are highly dependent on the substitution pattern of the indacene core, which allows the design of new dyes with improved optical properties ranging from the blue to the red region of the spectrum by appropriate selection of the electronic properties and positions of the substituents.[1] Core-halogenated BODIPYs are highly versatile starting materials for the modulation and optimization of these properties, facilitating the introduction of chemical diversity in the indacene nucleus through nucleophilic substitution of halogen[8] or through metal-catalyzed cross-coupling reactions.[2e,3m,4m,8l–8m,8o–8q,9] The chloro-BODIPYs have been the derivatives most widely used for this purpose, allowing the introduction of a wide range of C-, N-, O-, S-, Se-, and Te-based substituents.[4k,8a–8n,8p,9b,9e,9g,9s] Bromo- and iodo-BODIPYs have attracted interest in their own right as photosensitizers for solar hydrogen production[10] and as probes for PDT.[3] Iodine or bromine incorporation into the BODIPY core enhances intersystem crossing to the triplet excited state upon irradiation, as required for efficient singlet oxygen generation in PDT.

[a] Instituto Química-Física "Rocasolano", CSIC,
Serrano 119, 28006 Madrid, Spain
Fax: +34-915642431
E-mail: i.garcia-moreno@iqfr.csic.es
Homepage: http://www.iqfr.csic.es/ql/Web_QL/Laser_material.htm
[b] Departamento de Química Orgánica I, Facultad de Ciencias Químicas, Universidad Complutense,
28040, Madrid, Spain
Fax: +34-913944103
E-mail: mjortiz@quim.ucm.es
Homepage: http://www.ucm.es/info/quimorga/index_ENG.htm
[c] Departamento de Química Física, Universidad del País Vasco-EHU, Facultad de Ciencias y Tecnología,
Apartado 644, 48080 Bilbao, Spain
[d] Instituto de Química Orgánica General, CSIC,
Juan de la Cierva 3, 28006 Madrid, Spain
Fax: +34-915644853
E-mail: jl.chiara@iqog.csic.es
Homepage: http://www.iqog.csic.es/iqog/investigador/jose-luis-chiara-romero

Supporting information for this article is available on the WWW under http://dx.doi.org/10.1002/ejoc.201200946.

Conversely, in spite of the wide synthetic use of chloro-BODIPYs, their photophysical properties have scarcely been studied, possibly due to the expectation that chlorine substituents should impact negatively on both stability and fluorescence, owing to their high chemical reactivity and to the heavy atom effect.[11] Chlorine has, however, been reported to increase fluorescence in certain cases,[12] including some very recent examples of BODIPY dyes.[8d,8j,8m,9g,13] Accordingly, in this work we have synthesized a series of new BODIPY dyes bearing one to six chlorine atoms at different positions on the boradiazaindacene core (Scheme 1). This library of chlorinated BODIPYs allowed us to perform a detailed analysis, both from experimental and from theoretical points of view, of the dependency of the emitting properties of the dye on the number and positions of chlorine substituents on the BODIPY core. In the following section we describe the preparation of four different series of chlorinated BODIPY dyes together with a theoretical study of their structures and charge distributions, and finally we discuss the photophysical properties and laser behavior of the new dyes.

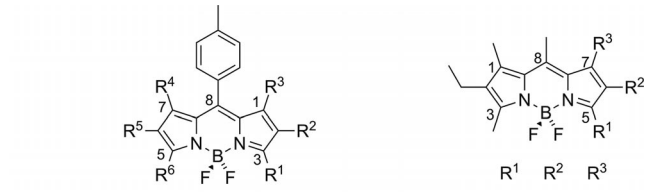

	R^1	R^2	R^3	R^4	R^5	R^6
1	H	H	H	H	H	H
2	H	Cl	H	H	H	H
3	H	Cl	H	H	Cl	H
4	Cl	H	H	H	H	Cl
5	Cl	Cl	H	H	H	Cl
6	Cl	Cl	H	H	Cl	Cl
7	Cl	Cl	Cl	Cl	Cl	Cl
8	4-C_6H_4CHO	H	H	H	H	4-C_6H_4CHO
9	4-C_6H_4CHO	Cl	H	H	H	4-C_6H_4CHO
10	4-C_6H_4CHO	Cl	H	H	Cl	4-C_6H_4CHO

	R^1	R^2	R^3
11	H	H	H
12	Cl	H	H
13	Cl	H	Cl
14	Cl	Cl	H

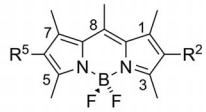

	R^2	R^5
15	H	H
16	Cl	H
17	Cl	Cl

Scheme 1. Core-chlorinated BODIPY dyes studied in this work and starting BODIPYs (**1**, **8**, **11**, **15**) used for their synthesis.

Results and Discussion

Synthesis

For the synthesis of the new chloro-BODIPYs we followed the three general strategies previously described for other halo-BODIPYs by electrophilic halogenation: a) direct halogenation of the unsubstituted BODIPY dye,[3c–3k,3m–3n,8o–8q,9c–9d,9f,9h,9o–9r,10,13a,14] b) halogenation of the dipyrromethane intermediate,[2e,8b,8e,8k,8n,9g,9l,9n,9t,15] and c) halogenation of the pyrrole precursors.[8j,8m,8p,9a,9e,9n]

The 2-mono-, 2,6-di-, 2,3,5-tri-, and 2,3,5,6-tretrachlorinated derivatives **2**, **3**, **5**, and **6**, respectively, were prepared by direct halogenation of BODIPY **1** with increasing amounts of *N*-chlorosuccinimide (NCS) as halogenating reagent (Scheme 2). Treatment of **1**[16] with NCS (2 equiv.) in THF at room temperature thus gave the 2-chloro-BODIPY **2**. No other monochlorinated derivatives were formed under the reaction conditions. Increasing the amount of NCS to 3 equiv. afforded the 2,6-dichloro-BODIPY **3** as major product (85%). Although it was possible to obtain the 2,3,5-trichloro derivative **5** by further increasing the amount of NCS to 4 equiv., the yield was low (32%), due to the concomitant formation of other polychlorinated products, including the 2,3,6-trichloro derivative, that could not be isolated pure. When 10 equiv. of NCS were used, the 2,3,5,6-tetrachloro-BODIPY **6** was obtained in 78% isolated yield. Use of larger amounts of NCS gave complex mixtures of polychlorinated products.

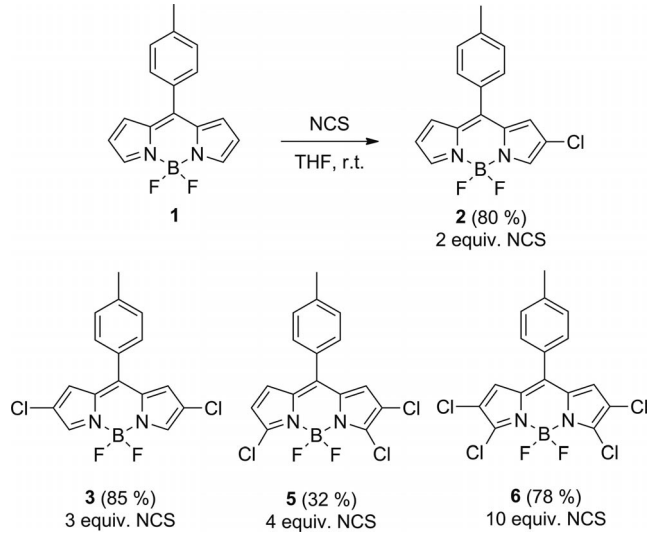

Scheme 2. Synthesis of BODIPYs **2**, **3**, **5**, and **6**.

For the preparation of 3,5-dichloro BODIPY **4**, we used the synthetic route described by Dehaen and Boens,[8b] starting from the corresponding dipyrromethane derivative **18**.[17] A similar strategy was employed for the synthesis of the hexachloro derivative **7** (Scheme 3), because this compound could not be isolated by direct halogenation of the BODIPY core, as mentioned above. Hexachlorination of **18**, requiring the use of a large excess (14 equiv.) of NCS at room temperature, was followed by oxidation of the chlorinated dipyrromethane with DDQ and subsequent treatment with $BF_3{\cdot}OEt_2$ in the presence of triethylamine to afford **7** in 30% overall yield.

Direct halogenation of BODIPY **11**[4l] gave a complex mixture of products that was very difficult to purify. In this case, halogenation of the pyrrole precursor was more appropriate (Scheme 4). 2-Acetylpyrrole was treated either with 1.1 or with 3 equiv. of NCS in THF at room temperature to give 2-acetyl-5-chloropyrrole (**19**)[8m,9e,18] or a mixture of 2-acetyl-3,5-dichloropyrrole (**20**) and 5-acetyl-2,3-dichloropyrrole (**21**),[18b] respectively, in moderate yields.

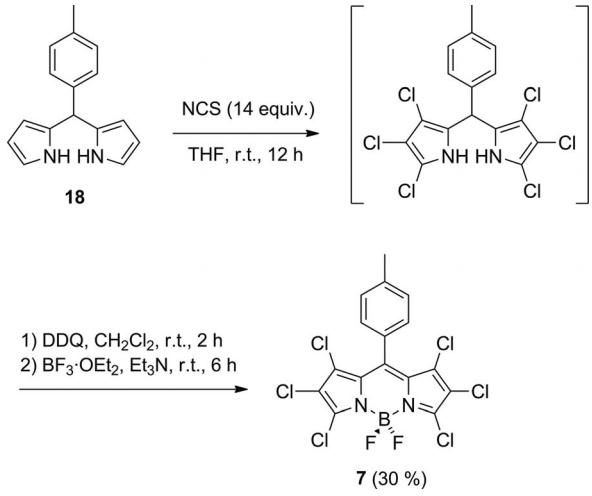

Scheme 3. Synthesis of hexachlorinated BODIPY **7**.

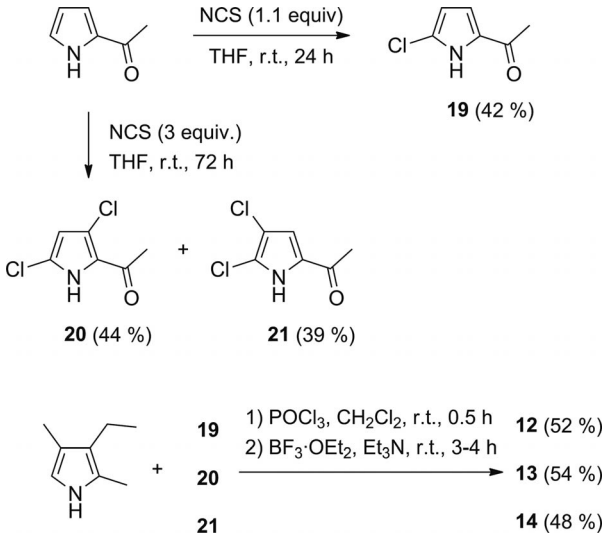

Scheme 4. Chlorination of 2-acetylpyrrole to generate BODIPY dyes **12**, **13**, and **14**.

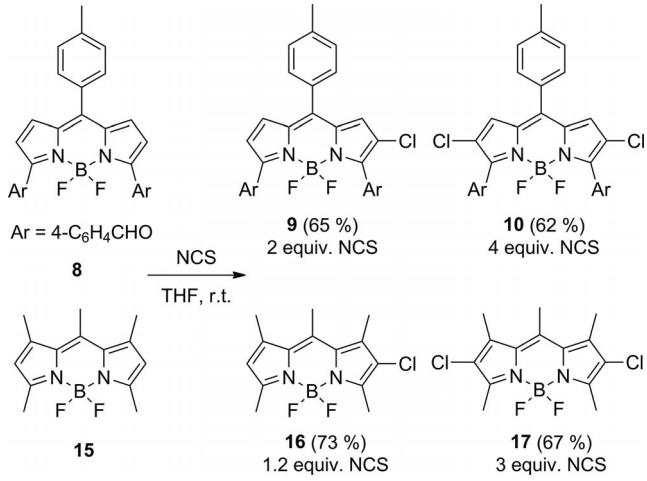

Scheme 5. Synthesis of BODIPYs **9**, **10**, **16**, and **17**.

Subsequent treatment of these pyrroles with 3-ethyl-2,4-dimethylpyrrole and phosphorus oxychloride, followed by treatment with $BF_3{\cdot}OEt_2$ in the presence of triethylamine, yielded the chlorinated BODIPY dyes **12** (52%), **13** (54%), and **14** (48%).

2-Chloro-BODIPY **9** and 2,6-dichloro-BODIPY **10** were obtained in good yields (62–65%) by direct chlorination of dye **8**[4k] with appropriate amounts of NCS (Scheme 5). A similar procedure was used for the preparation of compounds **16** (73%) and **17** (67%) starting from commercially available dye **15** (PM546, Scheme 5).

Theoretical Study

We calculated the charge distributions (CHelpg) of the new BODIPYs with the objective of understanding the regioselectivities of the electrophilic halogenation reactions (Table 1 and Figures S1–S4 in the Supporting Information). The charge distribution map of, for instance, the parent non-halogenated compound **1** indicates that the BODIPY chromophore is most susceptible to electrophilic attack by chlorine (Table 1) at the 2- and the 6-positions, which have the highest negative charge, consistently with experimental observations in the synthesis of mono- and dichlorinated dyes **2** and **3**.

Table 1. Potential electrostatic map (red denotes negative and blue positive charge) of compound **1** and CHelpg charge distributions for the chromophoric carbon atoms susceptible to electrophylic attack by chlorine in the ground states of its chlorinated derivatives **2**–**7**. The full data, including the excited states, are listed in Figure S1 in the Supporting Information.

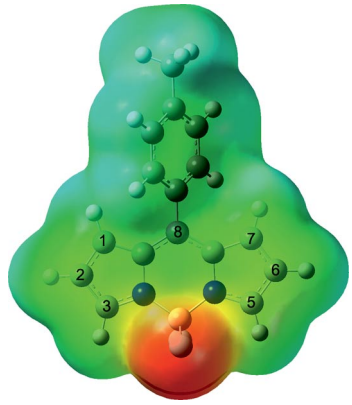

Dye	BODIPY carbon atoms					
	1	**2**	**3**	**5**	**6**	**7**
1	–0.109	–0.180	0.041	0.041	–0.179	–0.111
2	–0.107	–0.181	0.046	0.036	0.064	–0.150
3	–0.135	0.055	0.061	0.039	0.061	–0.131
4	–0.081	–0.201	0.200	0.197	–0.198	–0.082
5	–0.078	–0.181	0.189	0.168	0.055	–0.129
6	–0.112	0.043	0.171	0.173	0.040	–0.114
7	0.084	0.004	0.190	0.171	0.028	0.066

Upon substitution, the highly electronegative chlorine atom perturbs the charge distribution in the BODIPY framework, inducing a positive charge at the site of substitution and a negative charge at the adjacent carbon. As a

result, the positions most susceptible to further electrophilic substitution are now expected to be carbons 1 and 7 in preference to 3 and 5, according to their calculated charges. However, the opposite order of reactivity is observed for the chlorination reaction, probably as a consequence of the steric hindrance introduced by the tolyl substituent on the flanking CH carbons 1 and 7. Similar regioselectivity orders have been observed for stepwise brominations[8o] and iodinations[3n] of the same or closely related 8-arylated BODIPYs. In any case, use of large excesses of the halogenating reagents allows substitution at the 1- and the 7-positions.[8o]

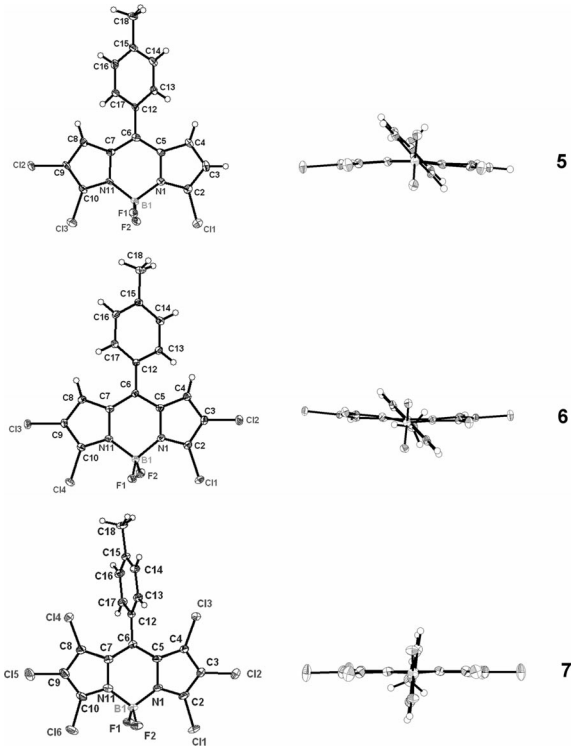

Figure 1. X-ray structures of BODIPY dyes **5**–**7**.

The optimized geometries predict that the 8-tolyl ring will be twisted with respect to the nearly planar indacene core, hampering electronic coupling between their electronic clouds. In all of the derivatives **2**–**6**, with free positions (1 and 7) adjacent to the aryl group, its rotation angle is about 55°, whereas the incorporation of chlorine at those positions (compound **7**) induces enough steric hindrance to twist the phenyl ring to a perpendicular disposition (89°) with respect to the chromophoric plane. These theoretical gas-phase predictions are in good agreement with the experimentally obtained (X-ray diffraction, solid state) geometries depicted in Figure 1. Indeed, the measured rotation angles are about 45° for compounds **5** and **6**, and 86° for derivative **7**. This concordance indicates that the calculated geometries are accurate.

Photophysical and Lasing Properties

Photophysics of Chlorinated 8-Tolyl-BODIPYs

The photophysical properties of this set of derivatives (Table 2) are governed by the presence of the tolyl unit at the *meso* position. In parent compound **1**, the absence of substituents at both *ortho* positions of the phenyl ring and/or the corresponding adjacent positions of the chromophoric system allows the unrestricted rotation of the aryl group.[19,20] Accordingly, the probability of internal conversion processes is greatly increased due to vibrational coupling, inducing drastic decreases both in fluorescence capability and in fluorescence lifetime, with respect to those exhibited by the fully unsubstituted BODIPY ($\phi \approx 0.90$ and $\tau \approx 7$–8 ns).[4o] In addition, the absence of the steric hindrance that would be required to constrain the phenyl ring in a perpendicular disposition could enable interaction with the BODIPY chromophore, distorting its planarity and further contributing to the nonradiative deactivation processes.[21,22]

Monochlorination of **1** at the 2-position and dichlorination at the 2- and 6-positions (dyes **2** and **3**, respectively) shift the spectral bands to lower energies and reduce the

Table 2. Photophysical properties of 8-tolyl-BODIPY (**1**) and its chlorinated derivatives **2**, **3**, and **5**–**7** in a common solvent (cyclohexane). The biexponential deconvolutions at the emission maxima are listed together with the amplitude-averaged lifetimes ($<\tau>$). The rate constants are calculated from these last values. The full photophysical data in several media are collected in Table S1 in the Supporting Information. The rate constants were calculated from the main lifetimes.

Dye	λ_{ab} [nm]	ε_{max} (f) [10^{-4} M^{-1} cm^{-1}]	λ_{fl} [nm]	ϕ	τ [ps]	$<\tau>$ [ps]	$<k_{fl}>$ [10^{-8} s^{-1}]	$<k_{nr}>$ [10^{-8} s^{-1}]
1	500.5	6.9 (0.42)	516.0	0.036	340 2285 (≈ 0 %)	340	1.05	28.3
2	518.5	6.5 (0.42)	534.5	0.093	845 (98%) 2255 (2%)	873	1.06	10.4
3	538.0	1.4 (0.11)	555.0	0.153	1320 (90%) 3860 (10%)	1574	0.97	5.38
5	530.0	10.5 (0.50)	542.0	0.56	2120 (12%) 4110 (88%)	3871	1.44	1.13
6	546.5	8.3 (0.54)	557.5	0.46	1180 (22%) 4720 (78%)	3941	1.16	1.37
7	537.0	9.5 (0.46)	548.5	0.45	1500 (10%) 2550 (90%)	2445	1.84	2.25

absorption probabilities, particularly in the latter case. Such trends are attributable to the electron-withdrawing effect of the electronegative chlorine atom, which removes electron density from the BODIPY core. The fluorescence quantum yields and lifetimes of the new dyes increase significantly with chlorination (Figure 2) as a consequence of the induced drastic reduction in nonradiative deactivation processes (Table 2 and Table S1 in the Supporting Information). In fact, the nonradiative rate constant decreases by about 50% for each chlorine atom incorporated on the BODIPY core. Moreover, further chlorination at the 3- and 5-positions to afford the tri- and tetrachlorinated derivatives **5** and **6** gives rise to a further and significant modification of the photophysical behavior, revealing that halogenation gives entirely different results depending on the positions at which the chlorine atoms are incorporated. Chlorination at the 3- and 5-positions thus leads to an important increase in the absorption probability (ε of dye **6** is six times higher than that of **3**), fluorescence quantum yield (ϕ of dye **6** is three times higher than that of **3**), and fluorescence lifetime, once more due to a drastic decrease in the nonradiative deactivation processes (Table 2 and Figure 2). In fact, the increases in the fluorescence capacities of dyes **5** and **6** cannot be associated with increases in the radiative rate constants, but with decreases in the nonradiative processes – $<k_{nr}>$ – varying from ca. 5×10^8 s^{-1} in dichlorinated **3** to ca. 1.2×10^8 s^{-1} in tri- and tetrachlorinated **5** and **6** (Table 2). Similar photophysical properties were reported by Boens et al. for compound **4**, with chlorine substituents at the 3- and 5-positions.[23] The same trends hold true for the fully chlorinated derivative **7**, although the spectral bands are in this case no longer shifted to lower energies, in spite of the larger number of chlorine atoms on the BODIPY core.

To provide an acceptable explanation for the dependence of the photophysical properties of these BODIPY derivatives on the numbers and positions of chlorine atoms, some considerations are to the point. Drexhage points out that C–H bond vibrations in the chromophore favor internal conversion processes and that the replacement of such bonds (e.g., by C–Cl bonds) should favor fluorescence emission.[24] However, such effects are rather small (i.e., <10%) and cannot explain the dependence of the fluorescence capacity on the position of the chlorine substituent in the BODIPY core. Charge transfer phenomena can also be ruled out because the photophysical properties are not very sensitive to the environment polarity (see Table S1 in the Supporting Information, in which the photophysical properties of the new dyes are analyzed as a function of the nature of the solvent). Moreover, electronic interaction between the phenyl ring and the chromophore as a consequence of the number of chlorine substituents can be discounted because the associated twist angles are almost the same in the different derivatives (around 55°, except in the case of the hexachlorinated compound **7**, in which this angle is 89°) and also in the different simulated solvents. The chlorination effect should therefore be related to its influence on the free motion of the 8-tolyl group, which is the key factor in the photophysics of this set of derivatives. A closer inspection of Table S1 in the Supporting Information reveals that the relationship between the fluorescence quantum yield and the degree of chlorination and anchoring position on the core is mainly governed by the probability of the nonradiative processes (internal conversion). The *meso* position in compound **1** is characterized by a high electronic density in the LUMO state and, consequently, it should be very sensitive to substituent effects.[4a] The removal of electronic density from the central position bearing the tolyl substituent by the electronegative chlorine substituents should thus be beneficial for the fluorescence capabilities of the chlorinated derivatives because it should significantly reduce the deleterious influence of the phenyl free rotation on their photophysics. In this way, the chlorinated derivatives show behavior similar to that previously observed for long-wavelength 8-tolyl-BODIPY dyes, in which electron density withdrawal from the chromophore core by extended π-conjugation through 3- and 5-aromatic substituents significantly reduced the influence of the free motion of the 8-tolyl group and led to highly efficient red-emitting BODIPYs.[4k] Although this effect is already

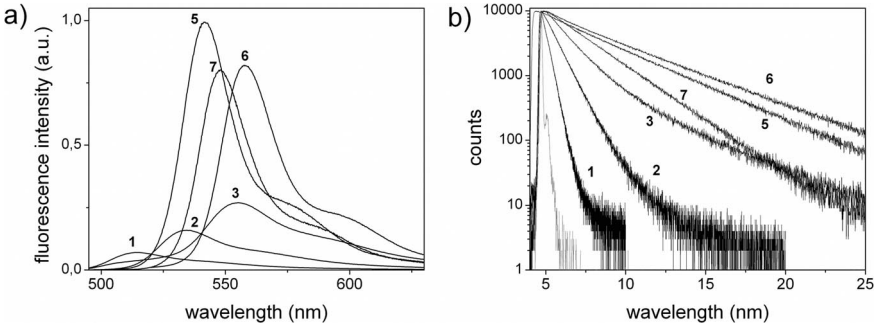

Figure 2. a) Fluorescence spectra of 8-tolyl-BODIPY (**1**) and its mono- (**2**), di- (**3**), tri- (**5**), tetra- (**6**), and hexachlorinated (**7**) derivatives, scaled by their fluorescence capabilities in cyclohexane, on excitation at the vibrational shoulder at lower energies. b) Corresponding fluorescence decay curves of these dyes.

achieved on incorporation of chlorine atoms at the 2- and 6-positions of the BODIPY core (compounds **2** and **3**), it becomes more relevant in dyes **4**–**7**, in which the 3- and 5-positions are also chlorinated.

This behavior is also confirmed by the biexponential character acquired by the fluorescence decay curves (monitored at the maximum of the emission spectrum) with chlorination. Whereas the fluorescence decay of the parent dye **1** is essentially a monoexponential curve characterized by a very short lifetime (<500 ps), monochlorination (dye **2**) already induces a biexponential decay, lengthening the short lifetime (ca. 800 ps) and giving rise to a longer one (ca. 2–3 ns). The contributions and durations of this component increase progressively with the number of chlorine atoms: from ca. 10% and 3.8 ns, respectively, in dye **3** up to ca. 80% and 4.7 ns, respectively, in tetrachlorinated dye **6**. This biexponential deconvolution was confirmed at different emission wavelengths, covering the whole fluorescence spectrum (see Table S2 in the Supporting Information). If the decay curves are monitored at the edges of the emission spectrum, the contributions of the short lifetimes are increased. Such biexponential behavior suggests the presence of two interconverting excited states. According to previously reported theoretical modeling of the excited states of 8-aryl-substituted BODIPYs, the phenyl ring can adopt two different conformations in the exited state: twisted and coplanar with respect to the BODIPY core, due to its unrestricted rotation.[21,22] Unfavorable steric interactions in the coplanar conformer cause an out-of-plane distortion of the indacene framework, this being a non-fluorescence state. The short (<1 ns) and the long (ca. 4 ns) components of these lifetimes should hence be assigned to fluorescence strongly reduced by the free motion of the 8-tolyl group, which makes electronic coupling between the phenyl group and the BODIPY core feasible, and to the normal emission of the BODIPY dye, because it reaches values typical of these chromophores, respectively.[4a] It seems that the emission bands of the coplanar states (poorly fluorescent) should be broader than those of the twisted states (mainly responsible for the fluorescence signal), explaining why the contributions of the short lifetimes to the decay curves are higher at the edges of the emission spectra. Similar trends have previously been reported for the decay curves of analogues bearing iodine atoms.[3n] In fact, the fluorescence capabilities of the chlorinated derivatives increase simultaneously with the contributions and lengthenings of this second components in the corresponding fluorescence decay curves (Figure 2), in accordance with lower populations or influence of the coplanar quenching excited states.

The simulated charge distributions (CHelpg) of all these chlorinated derivatives confirm the above hypothesis (Figure S1 in the Supporting Information). In general, the presence of the highly electronegative chlorine atom induces a charge redistribution in the BODIPY core, in which the carbon bonded to chlorine acquires a strong positive charge while the adjacent ones become more negatively charged and, consequently, the positive charges of the neighboring carbons are increased. Such effects are softened at the BODIPY carbon atoms further separated from the chlorinated one. As would be expected, the charge rearrangements induced by chlorination increase with the number of chlorine atoms, always being more significant in the excited states, in which the electronic motion is favored. In addition, substitution at the terminal positions of the delocalized π-systems (the 3- and 5-positions) favors electronic delocalization, especially in the excited states (Figure 3 and Supporting Information, Figure S1), efficiently removing the electronic density from the *meso* positions (in S_1 from 0.135 in compound **1** to 0.270 in tetrachlorinated **6**) and, consequently, significantly reducing the deleterious effect of the 8-tolyl motion on the photophysics. This "push-pull" effect[3n,16] causes the significant increases observed both in the absorptions and in the fluorescence probabilities of dyes **5**–**7**. Such charge rearrangement upon excitation should be the reason for the lack of correlation between the molar absorptions and the radiative deactivation rate constants.

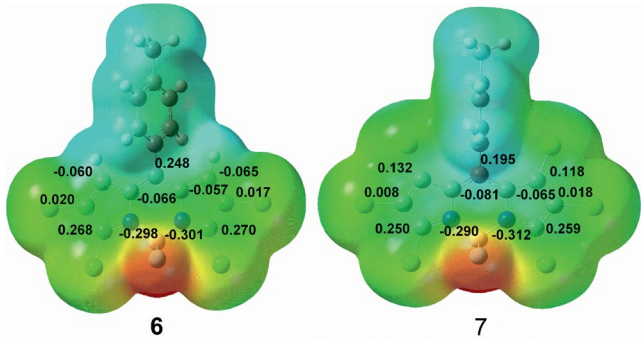

Figure 3. Potential electrostatic maps (red denotes negative and blue positive) together with the CHelpg charge distributions in the excited states for tetra- (**6**) and hexachlorinated (**7**) dyes. The whole charge distributions in ground and excited states are listed in Figure S1 in the Supporting Information.

At this point, it should be noted that, according to theoretical calculations, chlorination does not imply a significant modification in the dihedral angle of the 8-phenyl group with respect to the BODIPY plane (Figure 3, 55°). Therefore, the smaller influence of the free motion of the phenyl group on the photophysics of the chlorinated derivatives is only due to the significant reductions in the electronic charge density at the *meso* positions. On the other hand, the incorporation of chlorine atoms at the 1- and 7-positions of the BODIPY framework, adjacent to the tolyl group, has the opposite effect, concentrating electronic charge around the *meso* positions and enhancing the influence of aryl rotation. Indeed, a direct comparison of the charge distributions of compounds **7** and **6** indicates that the electronic charge at the *meso* position is less positive in the former (0.195 and 0.248, respectively, Figure 3). However, in the case of dye **7**, the steric hindrance induced by the chlorine atoms alters the orientation of the phenyl ring with respect to the indacene plane, and places it nearly perpendicular (Figures 1 and 3, 86° from X-ray and 89° from theoretical calculations, respectively). In this arrangement, the phenyl free motion is hindered and dye **7** exhibits a fluorescence capability similar to that of dye **6**.

Photophysics of Chlorinated Red-Emitting-BODIPY Dyes

The above hypothesis about the electron-withdrawing effect of chlorine on the free rotation of the 8-aryl group was confirmed by analysis of the influence of chlorination on the photophysics of the red-emitting BODIPY **8** (Scheme 5<xshr5>), with the 3- and 5-positions substituted with *p*-formylphenyl groups.[4k] In this derivative **8**, which also bears a tolyl group at the *meso* position, the deleterious influence of this aryl free motion on the fluorescence emission is minimized by the delocalization of the π-system through the aromatic substituents at the 3- and 5-positions.[4k] Consequently, the chromophoric electronic density is removed from the *meso* position, explaining its high fluorescence quantum yield in relation to that of parent compound **1** (see the charge distributions in Figures S1 and S2 in the Supporting Information). Dye **8** was mono- (compound **9**) and dichlorinated (compound **10**) at the 2- and 6-positions (Scheme 5), as predicted by quantum mechanical calculations, which revealed that these positions have the highest negative charges in the chromophore and are hence the most susceptible to electrophilic attack (Figure S2 in the Supporting Information). The corresponding photophysical data in a common solvent are collected in Table S3 in the Supporting Information.

Figure 4 shows that chlorination of dye **8** induces further shifts of its bands to the red, as well as a decrease in the absorption probability in the dihalogenated derivative (from 3.3×10^4 M^{-1}cm^{-1} in **8** to 1.1×10^4 M^{-1}cm^{-1} in **10**). Moreover, the fluorescence quantum yields also decrease (from 0.54 to 0.42 upon the first halogenation to 0.39 after attachment of the second chlorine atom), through reductions in the radiative deactivation rate constants and increases in the internal conversion probabilities (Table S3 in the Supporting Information). In the previous set of derivatives **1**–**7**, the chlorine electron-withdrawing effect enhances the fluorescence emission by decreasing the internal conversion associated with the 8-tolyl motion. In the case of compounds **8**–**10**, however, such a nonradiative pathway is already counteracted by the aromatic substitution at the 3- and 5-positions, so the high electronegativity of the chlorine atom decreases the π-delocalization of the BODIPY through the 3- and 5-aromatic substituents, causing the observed reductions in the absorption and emission probabilities of dyes **9** and **10** with respect to the non-chlorinated dye **8**. Moreover, the further shifts of the spectral bands to lower energies upon chlorination imply that their excited and ground states are energetically closer and that, accordingly, the internal conversion processes are enhanced in terms of the energy gap law, which works well for dyes emitting in the red part of the visible.[25–28]

Photophysics of Chlorinated Alkyl-BODIPY Dyes

To gain further insights into the effect of chlorination on the photophysics of BODIPY dyes, we studied cases of alkyl-substituted BODIPYs. We selected the previously reported compound **11**[4l] (Scheme 1) and the well-known commercial dye PM546 (**15**, Scheme 5).[29] The corresponding photophysical data in a common solvent are collected in Table 3.

Table 3. Photophysical properties of compounds **11** and **15** and of their mono- and dichlorinated derivatives (**12–14** and **16–17**, respectively) in cyclohexane. The full photophysical data in all the solvents studied are included in Tables S4 and S5, respectively, in the Supporting Information.

Dye	λ_{ab} [nm]	ε_{max} (f) [10^{-4} M^{-1} cm^{-1}]	λ_{fl} [nm]	ϕ	τ [ns]	k_{fl} [10^{-8} s^{-1}]	k_{nr} [10^{-8} s^{-1}]
11	504.0	3.3 (0.22)	515.0	0.96	5.46	1.75	0.07
12	510.5	5.1 (0.33)	520.5	0.78	5.07	1.54	0.43
13	504.0	3.3 (0.27)	526.0	0.57	3.95	1.44	1.09
14	521.0	3.3 (0.24)	531.0	0.83	5.29	1.57	0.32
15	499.5	9.7 (0.50)	512.0	0.91	5.23	1.74	0.17
16	512.0	5.5 (0.26)	525.5	0.91	5.54	1.64	0.16
17	527.0	7.1 (0.34)	542.5	0.87	5.65	1.54	0.23

In this set of derivatives the fluorescence decay curves are satisfactorily analyzed as monoexponentials, thus corroborating the influence of the aryl ring on the appearance of second exponentials for the derivatives **1**–**7** discussed above. The reference compound **11** is characterized by an asymmetric substitution pattern of the pyrroles, one being fully alkylated and the other fully unsubstituted. The incorporation of chlorine at the 5-position (compound **12**) increases the absorption probability, in accordance with the push-pull effect postulated above, but decreases the fluorescence capability of the dye. Both the reference dye **11** and

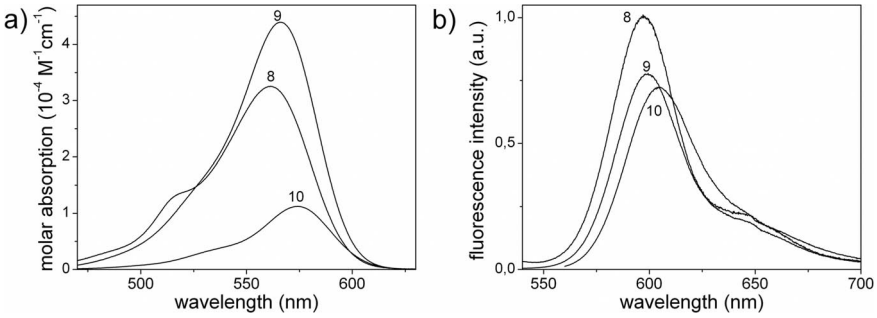

Figure 4. a) Absorption and b) fluorescence spectra of compound **8** and of its mono- (**9**) and dichlorinated (**10**) derivatives scaled by their molar absorptions and fluorescence abilities, respectively, in cyclohexane.

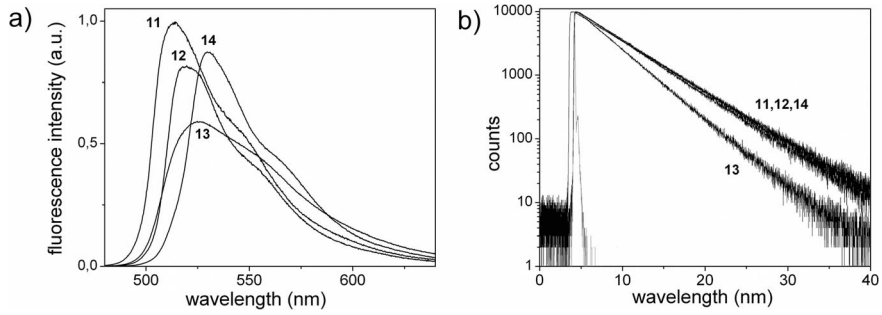

Figure 5. a) Fluorescence spectra of compound **11** and of its mono- (compound **12**) and dichlorinated derivatives **13** and **14**, scaled by their fluorescence capabilities in cyclohexane. b) Corresponding fluorescence decay curves of these dyes.

its monochlorinated derivative **12** exhibit only slight sensitivities to solvent (see Table S4 in the Supporting Information), with the fluorescence quantum yields decreasing only slightly on going from cyclohexane (0.96 for **11** and 0.78 for **12**) to 2,2,2-trifluoroethanol (0.75 for **11** and 0.55 for **12**). This could be attributable to the asymmetric substitution patterns of the pyrroles, with the alkylated ones behaving as electron donors and the unsubstituted or halogenated ones as electron acceptors, giving rise to asymmetric charge distributions between the pairs of pyrrole rings in the BODIPY frameworks that enhance nonradiative deactivation processes mainly in polar media.

Further halogenation produces entirely opposite results depending on the positions at which the chlorine is attached. Whereas chlorination at the 5- and 6-positions (compound **14**) causes a larger shift to lower energies and a slight recovery of the fluorescence capability (Figure 5), chlorination at the 5- and 7-positions (compound **13**) induces just the opposite effect (i.e., a shift to higher energies and a further reduction in the fluorescence capability). Such opposed tendencies are mainly related to nonradiative processes (Table 3), because the asymmetry in the pyrrole charge distribution mentioned above (Figure S3) is more pronounced upon substitution at the 7-position than at the 6-position.

In the case of dye PM546 (**15**), monochlorination (compound **16**) keeps the typical fluorescence quantum yield of the BODIPY chromophore, with values very close to unity (Table 3 and Supporting Information, Table S5). Dichlorination (compound **17**) produces more pronounced electron removal from the chromophore and a consequent slight decrease in the fluorescence ability, in good agreement with previous results reported for BODIPYs bearing electron acceptor moieties.[30] As discussed above, the 2- and 6-positions are not very sensitive to substituent effects (Figure S4 in the Supporting Information), so, apart from the expected spectral shift to lower energies, the optimal fluorescence behavior of this BODIPY is preserved upon chlorination.

Lasing Properties

The lasing behavior of the *p*-tolyl chlorinated dyes **2**–**7** shows good correlation with their photophysical properties: the higher the fluorescence quantum yield, the higher the lasing efficiency, and the lower the nonradiative rate constant, the higher the lasing photostability.

Although the parent dye **1** does not lase, its chlorinated derivatives exhibit unexpected but highly efficient and photostable laser emission centered at ca. 575 nm when placed in a simple plane-plane nontunable resonator with a pump threshold energy of 0.8 mJ, a beam divergence of 5 mrad, and a pulse duration of 8 ns full-width at half maximum (FWHM). The dependence of the laser action of these new chlorinated derivatives on the corresponding dye concentrations was analyzed in ethyl acetate solutions by varying the optical densities from 8 to 30, while keeping all other experimental parameters constant. As an example, the results obtained for di- and trichlorinated dyes **3** and **5** are shown in Figure S5 in the Supporting Information.

Using the dye concentrations that optimized the laser efficiency of each derivative, we analyzed the dependence of their lasing properties both on the number and on the positions of the chlorine atoms attached to the chromophore. The laser efficiencies increase significantly with increasing chlorination of the BODIPY core, from 30% in monochlorinated dye **2** up to 60% in hexachlorinated dye **7** (Table 4). Consistently with the photophysical properties, chlorination at the 3- and 5-positions (dye **4**) enhances the laser efficiency with respect to that observed for dye **3**, which is also a dichlorinated derivative but with different regiochemistry (substituted at the 2- and 6-positions).[23]

The experimentally observable solvent effects on the dye laser action were analyzed in solutions of polar aprotic and polar protic solvents. No apolar solvents such as cyclohexane were used, due to the low solubilities of these new dyes, which prevented the production of solutions with the high dye concentrations required for laser operation under the pumping conditions selected in this work. Once again, photophysical and lasing properties are correlated: the higher the fluorescence quantum yields, the higher the lasing efficiencies. The laser actions of these chlorinated dyes in polar solvents such as acetone and methanol are thus less efficient than those registered in ethyl acetate. The *p*-tolyl chlorinated derivatives lase with high efficiencies, independently of the nature of the solvent (Table 4). These efficiencies are quite surprising in view of the low fluorescence quantum yields exhibited by these dyes (e.g., dye **2** lases with an efficiency of 28% in methanol in spite of having a fluorescent

Table 4. Lasing properties[a] of the new chlorinated derivatives of the *p*-tolyl BODIPY dye **1** in several solvents upon excitation at 532 nm.

Dye	Data	EtOAc	MeOH	Acetone	CH_2Cl_2
2[b]	λ_l [nm]	572	571	569	575
	Eff [%]	30	28	17	28
	I [%]	90			
3[c]	λ_l [nm]	575	574	575	580
	Eff [%]	44	38	29	40
	I [%]	95			
4[d]	λ_l [nm]	572	570	568	574
	Eff [%]	48	42	37	44
	I [%]	100			
5[e]	λ_l [nm]	573	570	567	569
	Eff [%]	58	49	48	53
	I [%]	100			
6[f]	λ_l [nm]	575	570	568	574
	Eff [%]	57	46	51	47
	I [%]	100			
7[g]	λ_l [nm]	571	569	568	569
	Eff [%]	60	49	52	51
	I [%]	100			

[a] *Eff*: energy conversion efficiency. λ_l: peak wavelength of the laser emission. *I*: intensity of the dye laser output after 100000 pump pulses with respect to its initial intensity I_0. $I(\%) = (I/I_0) \times 100$, at 10 Hz repetition rate. [b] Dye concentration: 5×10^{-3} M. [c] Dye concentration: 9×10^{-4} M. [d] Dye concentration: 9×10^{-4} M. [e] Dye concentration: 2×10^{-3} M. [f] Dye concentration: 5×10^{-4} M. [g] Dye concentration: 8×10^{-4} M.

quantum yield of only 0.044). This behavior might be related to the short fluorescence lifetimes observed in the chlorinated derivatives, which lead to radiative rate constants similar to those observed in other BODIPY dyes.[4k,4l]

The lasing photostabilities of these dyes in ethyl acetate solutions were also analyzed by the protocol described in the Exp. Section. To compare the effect of chlorination on this laser parameter properly, the photostability of the parent dye **1** was also analyzed, because although it does not lase, it was possible to follow the evolution of its laser-induced fluorescence as a function of the number of pump pulses. The results are reported in Table 4 and, for purposes of clarity, the actual patterns of the fluorescence emissions of dyes **1**, **2**, and **6** under pumping at a repetition rate of 10 Hz are plotted in Figure 6. Once again, chlorination enhances the performances of these dyes: even monochlorinated **2** is more photostable than the parent compound **1**, and the photostabilities increase with the number of chlorine substituents in the BODIPY core. The tri-, tetra-, or hexachlorinated derivatives are thus highly photostable dyes, maintaining their initial laser outputs without sign of degradation after 100000 pumping pulses at 10 Hz repetition rate even under the drastic pumping conditions selected in this work. Once again, this laser behavior can be explained well in terms of the photophysics, because chlorination decreases the nonradiative rate constants significantly (Table 2) and, consequently, increases the laser lifetimes.

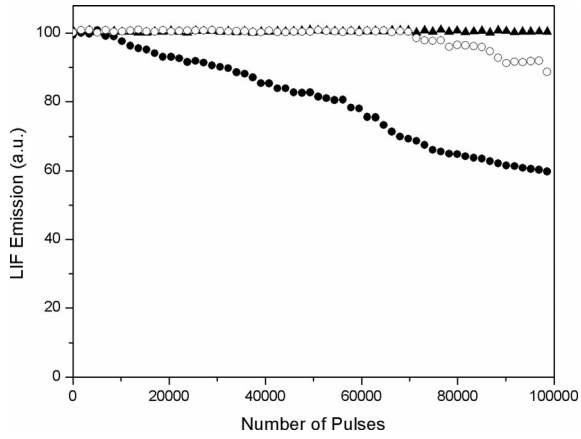

Figure 6. Normalized laser-induced fluorescence emissions as a function of the number of pump pulses for the dyes **1** (●), **2** (○), and **6** (▲) in ethyl acetate solutions. Pump laser wavelength, energy, and repetition rate: 532 nm, 5.5 mJ per pulse, and 10 Hz.

This enhancement of the laser behavior is also observed for all the other chlorinated BODIPY dyes **9** and **10** (derived from **8**), **12**–**14** (derived from **11**), and **16** and **17** (derived from **15**), when pumped under identical experimental conditions (Table 5). Dye **10**, for instance, exhibits a laser efficiency of 30% in ethyl acetate solution, which is a twofold increase with respect to its non-chlorinated parent dye **8**. The effect of chlorination on the laser actions of dyes **11** and **15** is outstanding. The low absorptions of parent dyes **11** and **15** at 532 nm preclude pumping at this standard wavelength. In fact, dye **11** has to be pumped at its maximum absorption wavelength (500 nm), increasing the technological complexity of the experimental setup and therefore limiting its applicability. The commercial dye PM546 (**15**) has to be pumped at a blue-shifted wavelength (355 nm), which is another standard wavelength used to induce laser emission from dye molecules. An advantage of chlorination of these dyes is the red-shifting of their absorption bands, allowing efficient pumping of the chlorinated derivatives at 532 nm, in the case of dye **11**, and even at

Table 5. Lasing properties of the new chlorinated BODIPY dyes in ethyl acetate solution pumped at 532 nm. For purposes of comparison, the corresponding data for the non-chlorinated dyes **8**, **11**, and **15**, evaluated under identical experimental conditions, are also included. Dye **11** was pumped at 500 nm and dyes **15** and **16** were pumped at 355 nm (data in parentheses).

Laser data	Dyes **8**[a]	**9**[b]	**10**[c]	**11**[d]	**12**[e]	**13**[e]	**14**[e]	**15**[f]	**16**[f(g)]	**17**[h]
Eff [%]	14	28	30	(34)	38	46	36	(23)	40 (30)	51
λ_l [nm]	615	612	618	(530)	561	566	562	(541)	558 (556)	562
I [%]	50	85	100	(80)	100	100	100	(60)	90	100

[a] Dye concentration: 1×10^{-3} M. [b] 8×10^{-4} M. [c] 1×10^{-3} M. [d] 6×10^{-4} M. [e] 15×10^{-3} M. [f] 25×10^{-3} M. [g] 3×10^{-3} M. [h] 3.5×10^{-3} M.

both standard wavelengths (355 and 532 nm) in the case of dye **15**. The monochlorinated derivative **12** thus lases at 561 nm with an efficiency of 38%, which increases to 46% for dichlorinated **13**. Similarly, monochlorinated **16** exhibits a highly efficient laser emission in ethyl acetate when pumped either in the UV or in the visible spectral regions. Whereas PM546 lases at 541 nm with an efficiency of 23% when pumped at 355 nm, its monochlorinated derivative **16** lases at 556 nm with an efficiency of 30% at the same pumping wavelength, which increases to 40% upon pumping at 532 nm.

Similar enhancement of the laser performances of dyes **8**, **11**, and **15** is also observed when the lasing properties of their chlorinated derivatives are analyzed as functions of the solvent (see Table S6 in the Supporting Information). In the same way, the photostabilities of these dyes are significantly improved by chlorination, the effect on the behavior of dye **8** being particularly remarkable; the laser output of **8** has decreased by 50% after 100000 pump pulses, but the presence of chlorine atoms is enough to maintain the laser emission at 100% of its initial value under the same experimental conditions.

Contrary to the behavior previously observed for the chlorinated derivatives of parent dye **1**, the laser data for chlorinated derivatives of **8**, **11**, and **15** do not correlate with their photophysical properties. In these dyes, the presence of chlorine induces significant increases in the laser actions (efficiencies and photostabilities) although, as discussed above, it has a deleterious effect on the photophysical properties (Tables S3–S5 in the Supporting Information) with the fluorescence quantum yields decreasing and the nonradiative rate constants increasing in relation to those registered for the non-chlorinated parent dyes.

A careful analysis of the results recorded with all the chlorinated BODIPY derivatives synthesized in this work suggests important questions about the influence of chlorine on the laser action of these dyes related to the following facts: a) a dye, such as tetrachlorinated **6**, with a fluorescence quantum yield in ethyl acetate as low as 0.39, exhibits a laser efficiency as high as 57%, b) a monochlorinated dye such as **12**, with a fluorescence quantum yield of 0.64, which is higher than that of **6**, exhibits a much lower laser efficiency (38%), c) monochlorinated laser dye **16**, with the highest fluorescence quantum yield (0.94), is not the most efficient laser dye of the series, and d) the good correlations established between the laser action and the photophysical properties of the chlorinated dyes derived from the parent compound **1** are not adhered to by the chlorinated dyes derived from compounds **8**, **11**, and **15**.

To gain deeper insight into the dependence of the laser behavior on chlorine substitution, we considered the effect of the polarization of the pump laser beam on the laser emissions of these new dyes, because the presence of an element as electronegative as chlorine should induce high dipole moments, the orientations of which would depend strongly on the number and positions of chlorine atoms on the BODIPY core. In the case of a dye molecule, the influence of polarization is determined mainly by the polarization of the exciting laser beam, the relative orientation of the transition moments in the dye molecule for the pumping and laser transitions, and the rotational diffusion-relaxation time. Matching the polarization of the pump laser to the preferred polarization of the gain medium can enhance the photon efficiency of the system. In contrast, if the applied field is not properly polarized or oriented with respect to the molecular dipole moment, the observed response will be reduced. To this end, the modules and orientations of the dipole moments of these molecules in the ground and excited states and the corresponding transition moments of absorption and emission were calculated (see Figures S6–S9 in the Supporting Information). The calculations showed that the transition moments of absorption and emission of the dye molecules studied are parallel to each other for excitation in the visible region of the spectrum because the same electronic transition is involved. The dye laser emissions were then measured as a function of the relative orientation between the polarization of the pumping radiation and that of the dye molecules. The pump laser was horizontally or vertically polarized by placing a combination of polarizer and $\lambda/2$ plate in the optical path. It was found that the tetrachlorinated dye **6**, which has a high dipole moment (11.230 D) totally aligned along (or parallel to) the transversal axis of the molecule, leads to a nonpolarized and highly efficient laser emission, regardless of the pump radiation being horizontally or vertically polarized.

With regard to dye **8**, its monochlorination to give **9** allows a better alignment of the molecular dipole moment along the transversal axis, reducing the twist angle of the dipole moment with respect to the axis induced by the *p*-formylphenyl substituent groups, which are disposed symmetrically, but slightly rotated with respect to the BODIPY core (Figure S8 in the Supporting Information) For this reason, dye **9** exhibits a nonpolarized laser emission with efficiency higher than that of its parent dye **8** and with a higher fluorescence quantum yield.

The influence of polarization on the laser actions of chlorinated dyes **12**, **14**, and **16** is more drastic, with dipole moments much lower and more rotated with respect to the transversal axis than those exhibited by the other chlorinated derivatives discussed previously (Figure S8 in the Supporting Information). Consequently, their laser emissions are highly polarized and, although efficient, are not as high as could be expected for dyes with the highest fluorescence quantum yields (0.78, 0.83, and 0.94, respectively).

The encouraging results registered with these new chlorinated dyes in the liquid phase led us to analyze the laser behavior of some of them when incorporated into solid-state matrices. The experiments were carried out with samples with those dye concentrations that had the highest lasing efficiencies in liquid solutions. MMA (methyl methacrylate) was chosen as the main monomeric component of the formulations because this ester mimics ethyl acetate, a solvent in which the studied dyes showed high lasing efficiencies. Broad-band and efficient laser emission, with beam divergence of ca. 5 mrad and pulse duration of ca. 5 ns FWHM, was registered for dyes **6** and **10** incorporated

as true solutions into the solid homopolymer PMMA (Table 6). No significant differences were observed in the wavelengths of the maximum laser emissions of each dye between their liquid and solid solutions. The dye-doped solid matrices exhibit high photostabilities, analyzed by monitoring the evolution of the laser outputs as a function of the number of pump pulses in the same position of the sample at a 10 Hz repetition rate. The lasing efficiencies of the solid materials (28% for **6** and 30% for **10**) are lower than those of the corresponding liquid solutions. Surface finishing of the solid samples in these experiments was not laser-grade, and higher lasing efficiencies would be expected with improved polishing.

Table 6. Laser properties of chlorinated BODIPY dyes **6** and **10** in PMMA pumped at 532 nm.

Dye	[Dye] (M)	*Eff* [%]	λ_l [nm]	*I* [%]
6	5.0×10^{-4}	28	565	100
10	1.1×10^{-3}	30	614	95

Conclusions

We have prepared a series of new mono- to hexachlorinated BODIPY dyes through three general synthetic strategies based on regioselective electrophilic chlorination with NCS as an inexpensive halogenating reagent. We have demonstrated that it is possible to control the degree of chlorination of the BODIPY core, which allows the synthesis of mono-, di-, and polychlorinated derivatives.

Quantum mechanical calculations can predict the positions at which chlorine will be incorporated and explain why some positions are less accessible to chlorination. Moreover, the positions at which the halogen is attached modulate the photophysical properties of the resulting BODIPYs. The fluorescence capacity of 8-tolyl-BODIPY or similar derivatives characterized by the presence of an aryl ring with unrestrained rotation can be tuned by the incorporation of appropriate substituents. In particular, the introduction of electron acceptor chlorine substituents at the 3- and 5-positions greatly increases the fluorescence capability of this compound. From a photophysical point of view, the chlorination of other BODIPYs leads to small reductions in fluorescence ability, but high fluorescence quantum yields are still obtained, making the use of these compounds as laser dyes possible.

The new chlorinated BODIPYs exhibit enhanced laser actions with respect to their non-halogenated analogues, both in liquid solution and in the solid phase. In fact, under demanding transversal pumping conditions, the presence of chlorine substituents allows lasing efficiencies as high as 60% to be reached, with high photostabilities. The surprisingly efficient laser actions from these newly chlorinated BODIPYs can be directly related to the improvement induced by chlorine in their photophysical properties and/or in their molecular dipole moments, increasing the modules and changing the orientations to match the polarization of the pump laser, which significantly enhances the photon efficiencies of the systems. In addition, chlorination is a facile and essentially costless protocol for overcoming important shortcomings exhibited by some commercial BODIPYs, such as low absorptions at standard laser pumping wavelengths and/or low photostabilities. In view of the easy synthetic assembly, and the large number of described BODIPY laser dyes, we are confident that this powerful approach can be extended to other dyes of this family, furthering their practical application in optical and sensing fields.[31]

Experimental Section

General: Starting materials and reagents used in the preparation of BODIPYs are commercially available unless their synthesis is described. The solvents were dried and distilled before use. Spectral data for the known compounds were in accordance with the literature data. Flash column chromatography was performed with silica gel (Merck 60, 230–400 mesh). ^{1}H and ^{13}C NMR spectra were recorded with a Bruker Avance DPX 300 spectrometer (300 MHz for ^{1}H and 75 MHz for ^{13}C) and a Bruker Avance III spectrometer (700 MHz for ^{1}H and 176 MHz for ^{13}C). All spectra were recorded in $CDCl_3$. ^{1}H chemical shifts are reported in ppm relative to tetramethylsilane (δ = 0.00 ppm) with use of the residual solvent signal as the internal reference. ^{13}C chemical shifts are reported in ppm with $CDCl_3$ (δ = 77.67 ppm) as the internal standard. IR spectra (cm^{-1}) were recorded with a Bruker Tensor 27 FTIR spectrophotometer. Melting points were determined in open capillaries and are uncorrected. High-resolution mass spectra were determined by ESI with a FTMS Bruker APEX Q IV instrument and by EI with a Thermofisher MAT 95 XP.

BODIPY dyes **1**,[16] **4**,[8b,23] **8**,[4k] and **11**[4l] were synthesized by the methods described previously. BODIPY **15** was purchased from Lasing, S.A. and used as received.

General Procedure for the Chlorination of BODIPY Core and Acetylpyrrole: NCS in dry THF was slowly added at room temp. to a solution of starting material in dry THF and the reaction mixture was stirred for 12–72 h under argon. The solvent was removed and the mixture was diluted with EtOAc, washed with aqueous HCl (10%) and H_2O, dried with $MgSO_4$, filtered, and concentrated to dryness. The halogenated compounds were purified by flash chromatography on silica gel.

General Procedure for the Synthesis of BODIPYs 12–14: $POCl_3$ (1.1 equiv.) was added to a solution of chlorinated 2-acetylpyrrole (1 equiv.) in $CHCl_3$, and the mixture was stirred for 30 min at room temp. 3-Ethyl-2,4-dimethylpyrrole (1 equiv.) in $CHCl_3$ was then added and the resulting solution was stirred for 12 h at room temp. Triethylamine (1 equiv.) was added, followed by $BF_3{\cdot}Et_2O$ (1 equiv.), and the mixture was stirred for 3–4 h before being quenched with aqueous HCl (10%) and extracted with CH_2Cl_2. The organic extracts were washed with water, dried with $MgSO_4$, and filtered, and the solvents were evaporated to dryness. The dyes were isolated and purified by flash chromatography on silica gel.

2-Chloro-4,4-difluoro-8-(4-tolyl)-4-bora-3a,4a-diaza-*s*-indacene (2): BODIPY **1** (50 mg, 0.18 mmol) in dry THF (20 mL) and NCS (47 mg, 0.36 mmol) in dry THF (5 mL) were allowed to react for 12 h. Flash chromatography with hexane/EtOAc (98:2) afforded **2** (45 mg, 80%) as a green-orange solid; m.p. 171.8–172.0 °C. ^{1}H NMR (700 MHz, $CDCl_3$): δ = 7.92 (s, 1 H, 5-H), 7.68 (s, 1 H, 3-

H), 7.39 (d, J = 8.4 Hz, 2 H, 2′-H), 7.28 (d, J = 8.4 Hz, 2 H, 3′-H), 6.95 (d, J = 4.2 Hz, 1 H, 7-H), 6.74 (s, 1 H, 1-H), 6.52 (d, J = 4.2 Hz, 1 H, 6-H), 2.41 (s, 3 H, CH_3) ppm. ^{13}C NMR (176 MHz, $CDCl_3$): δ = 147.8 (C-8), 145.8 (CH-5), 142.0 (C-4′), 139.7 (CH-3), 135.4 (C-7a), 133.2 (C-8a), 133.1 (CH-7), 130.6 (2×CH-2′), 130.5 (C-1′), 129.4 (2×CH-3′), 127.3 (CH-1), 121.5 (C-Cl), 119.3 (CH-6), 21.5 (CH_3) ppm. IR (neat): $\tilde{\nu}$ = 1548, 1405, 1364, 1259, 1105, 985 cm^{-1}. HRMS (ESI^+): calcd. for $[C_{16}H_{12}BClF_2N_2 + Na]^+$ 339.0648; found 339.0628.

2,6-Dichloro-4,4-difluoro-8-(4-tolyl)-4-bora-3a,4a-diaza-*s*-indacene (3): BODIPY **1** (40 mg, 0.14 mmol) in dry THF (15 mL) and NCS (56 mg, 0.42 mmol) in dry THF (5 mL) were allowed to react for 24 h. Flash chromatography with hexane/EtOAc (98:2) afforded **3** (39 mg, 85%) as an orange solid; m.p. 196.3–197.0 °C. ^1H NMR (700 MHz, $CDCl_3$): δ = 7.73 (s, 2 H, 3-H, and 5-H), 7.37 (d, J = 8.4 Hz, 2 H, 2′-H), 7.29 (d, J = 8.4 Hz, 2 H, 3′-H), 6.79 (s, 2 H, 1-H, and 7-H), 2.41 (s, 3 H, CH_3) ppm. ^{13}C NMR (176 MHz, $CDCl_3$): δ = 148.0 (C-8), 142.5 (C-4′), 141.8 and 141.7 (CH-3 and CH-5), 133.6 (C-7a and C-8a), 130.6 (2×CH-2′), 130.1 (C-1′), 129.6 (2×CH-3′), 128.6 and 128.5 (CH-1 and CH-7), 122.6 (C2-Cl and C6-Cl), 21.6 (CH_3) ppm. IR (neat): $\tilde{\nu}$ = 1550, 1484, 1358, 1261, 1112 cm^{-1}. HRMS (ESI^+): calcd. for $[C_{16}H_{11}BCl_2F_2N_2 + Na]^+$ 373.0258; found 373.0187.

2,3,5-Trichloro-4,4-difluoro-8-(4-tolyl)-4-bora-3a,4a-diaza-*s*-indacene (5): BODIPY **1** (90 mg, 0.32 mmol) in dry THF (15 mL) and NCS (171 mg, 1.28 mmol) in dry THF (10 mL) were allowed to react for 72 h. Flash chromatography with hexane/EtOAc (98:2) afforded **5** (40 mg, 32%) as an orange-red solid, together with an inseparable mixture of chlorinated products; m.p. 194.3–195.0 °C. ^1H NMR (700 MHz, $CDCl_3$): δ = 7.31 (d, J = 8.4 Hz, 2 H, 2′-H), 7.27 (d, J = 8.4 Hz, 2 H, 3′-H), 6.86 (d, J = 4.2 Hz, 1 H, 7-H), 6.74 (s, 1 H, 1-H), 6.41 (d, J = 4.2 Hz, 1 H, 6-H), 2.41 (s, 3 H, CH_3) ppm. ^{13}C NMR (176 MHz, $CDCl_3$): δ = 146.6 (C-8), 144.3 (C5-Cl), 142.0 (C-4′), 140.6 (C3-Cl), 134.1 (C-7a), 132.8 (CH-7), 131.1 (C-8a), 130.5 (2×CH-2′), 129.5 (2×CH-3′), 129.2 (C-1′), 127.2 (CH-1), 120.6 (C2-Cl), 119.6 (CH-6), 21.5 (CH_3) ppm. IR (neat): $\tilde{\nu}$ = 1554, 1387, 1258, 1107, 800 cm^{-1}. HRMS (ESI^+): calcd. for $[C_{16}H_{10}BCl_3F_2N_2 + Na]^+$ 406.9865; found 406.9834.

2,3,5,6-Tetrachloro-4,4-difluoro-8-(4-tolyl)-4-bora-3a,4a-diaza-*s*-indacene (6): BODIPY **1** (65 mg, 0.23 mmol) in dry THF (20 mL) and NCS (308 mg, 2.3 mmol) in dry THF (10 mL) were allowed to react for 48 h. Flash chromatography with hexane/EtOAc (98:2) afforded **6** (75 mg, 78%) as an orange-red solid; m.p. 231.0–231.8 °C. ^1H NMR (700 MHz, $CDCl_3$): δ = 7.30 (d, J = 8.4 Hz, 2 H, 2′-H), 7.28 (d, J = 8.4 Hz, 2 H, 3′-H), 6.79 (s, 2 H, 1-H and 7-H), 2.41 (s, 3 H, CH_3) ppm. ^{13}C NMR (176 MHz, $CDCl_3$): δ = 144.4 (C-8), 142.6 (C3-Cl and C5-Cl), 142.4 (C-4′), 131.4 (C-7a and C-8a), 130.5 (2×CH-2′), 129.6 (2×CH-3′), 128.9 (C-1′), 128.2 (CH-1 and CH-7), 121.6 (C2-Cl and C6-Cl), 21.5 (CH_3) ppm. IR (neat): $\tilde{\nu}$ = 1549, 1384, 1245, 1106 cm^{-1}. HRMS (EI): calcd. for $C_{16}H_9BCl_4F_2N_2$ 417.9579; found 417.9583.

1,2,3,5,6,7-Hexachloro-4,4-difluoro-8-(4-tolyl)-4-bora-3a,4a-diaza-*s*-indacene (7): NCS (3.38 g, 23.5 mmol) in dry THF (15 mL) was added slowly to a stirred solution of 5-(4-tolyl)dipyrromethane[17] (**18**, 400 mg, 1.69 mmol) in dry THF (30 mL), and the reaction mixture was heated at reflux under argon for 24 h. The solvent was removed, and DDQ (422 mg, 1.86 mmol) was added to the solution of the intermediate hexachlorodipyrromethane generated above in CH_2Cl_2 (50 mL). The mixture was stirred at room temp. for 1 h and triethylamine (1.5 mL, 8.4 mmol) was then added. After 10 min, $BF_3{\cdot}Et_2O$ (2 mL, 13.5 mmol) was added and the resulting solution was stirred for 24 h at room temp. The crude mixture was washed with H_2O, dried with $MgSO_4$, and filtered, and the solvents were evaporated to dryness. Purification by flash chromatography on silica gel with hexane/EtOAc (99:1) as eluent yielded **7** (245 mg, 30%) as a maroon solid; m.p. 275.1–276.0 °C. ^1H NMR (700 MHz, $CDCl_3$): δ = 7.26 (d, J = 8.4 Hz, 2 H, 2′-H), 7.06 (d, J = 8.4 Hz, 2 H, 3′-H), 2.40 (s, 3 H, CH_3) ppm. ^{13}C NMR (176 MHz, $CDCl_3$): δ = 143.7 (C-8), 142.5 (C-4′) 140.7 (C3-Cl and C5-Cl), 132.9 (C-7a and C-8a), 130.1 (2×CH-2′), 127.7 (2×CH-3′), 127.6 (C-1′), 126.3 (C1-Cl and C7-Cl), 121.4 (C2-Cl and C6-Cl), 21.6 (CH_3) ppm. IR (neat): $\tilde{\nu}$ = 1552, 1383, 1246, 1108 cm^{-1}. HRMS (ESI^-): calcd. for $[C_{16}H_7BCl_6F_2N_2 + CH_3OH - H]^+$ 518.8964; found 518.8926.

2-Chloro-4,4-difluoro-3,5-bis(4-formylphenyl)-8-(4-tolyl)-4-bora-3a,4a-diaza-*s*-indacene (9): BODIPY **8** (80 mg, 0.16 mmol) in dry THF (15 mL) and NCS (43 mg, 0.32 mmol) in dry THF (10 mL) were allowed to react for 48 h. Flash chromatography with hexane/EtOAc (9:1) afforded **9** (55 mg, 65%) as a red solid; m.p. 182.4–182.9 °C. ^1H NMR (700 MHz, $CDCl_3$): δ = 9.99 (s, 1 H, CHO), 9.95 (s, 1 H, CHO), 7.91 (d, J = 8.4 Hz, 2 H, 4-formylphenyl), 7.90 (d, J = 8.4 Hz, 2 H, 4-formylphenyl), 7.83 (d, J = 8.4 Hz, 2 H, 4-formylphenyl), 7.79 (d, J = 8.4 Hz, 2 H, 4-formylphenyl), 7.44 (d, J = 8.4 Hz, 2 H, 4-tolyl), 7.32 (d, J = 8.4 Hz, 2 H, 4-tolyl), 6.99 (d, J = 4.2 Hz, 1 H, 7-H), 6.87 (s, 1 H, 1-H), 6.66 (d, J = 4.2 Hz, 1 H, 6-H), 2.44 (s, 3 H, CH_3) ppm. ^{13}C NMR (176 MHz, $CDCl_3$): δ = 191.9 (CHO), 191.7 (CHO), 158.9 (C), 151.3 (C), 146.2 (C), 141.8 (C), 137.5 (C), 137.4 (2 C), 136.7 (C), 136.6 (C), 135.5 (C), 133.1 (CH), 131.1 (2×CH), 131.0 (C), 130.7 (2×CH), 130.0 (2×CH), 129.6 (2×CH), 129.4 (2×CH), 129.2 (2×CH), 127.8 (CH), 122.1 (C-Cl), 121.9 (CH) ppm. IR (neat): $\tilde{\nu}$ = 2926, 2860, 1702, 1542, 1260, 1073, 800 cm^{-1}. HRMS (EI): calcd. for $C_{30}H_{20}BClF_2N_2O_2$ 524.1272; found 524.1280.

2,6-Dichloro-4,4-difluoro-3,5-bis(4-formylphenyl)-8-(4-tolyl)-4-bora-3a,4a-diaza-*s*-indacene (10): BODIPY **8** (80 mg, 0.16 mmol) in dry THF (15 mL) and NCS (85 mg, 0.64 mmol) in dry THF (10 mL) were heated at reflux for 3 h. Flash chromatography with hexane/EtOAc (9:1) afforded **10** (55 mg, 62%) as a red solid; m.p. 211.3–211.8 °C. ^1H NMR (700 MHz, $CDCl_3$): δ = 9.98 (s, 2 H, 2×CHO), 7.87 (d, J = 7.7 Hz, 4 H, 3′-H), 7.75 (d, J = 7.7 Hz, 4 H, 2′-H), 7.44 (d, J = 8.4 Hz, 2 H, 2′′-H), 7.34 (d, J = 8.4 Hz, 2 H, 3′′-H), 6.93 (s, 2 H, 1-H and 7-H), 2.45 (s, 3 H, CH_3) ppm. ^{13}C NMR (176 MHz, $CDCl_3$): δ = 191.8 (2×CHO), 153.2 (C-3 and C-5), 146.4 (C-8), 142.2 (C-4′′), 136.8 (C-4′), 134.9 (C-1′), 133.4 (C-7a and C-8a), 130.9 (4 CH-2′), 130.6 (2×CH-2′′), 130.3 (C-1′′), 129.6 (2×CH-3′′), 129.2 (4 CH-3′), 129.1 (CH-1 and CH-7), 123.0 (C2-Cl and C6-Cl), 21.6 (CH_3) ppm. IR (neat): $\tilde{\nu}$ = 2924, 2856, 1700, 1540, 1268, 1219, 1144, 1070, 800, 768 cm^{-1}. HRMS (ESI^-): calcd. for $[C_{30}H_{19}BCl_2F_2N_2O_2 + CH_3OH - H]^+$ 589.1169; found 589.1234.

Chlorination of Acetylpyrrole: 2-Acetylpyrrole (200 mg, 1.83 mmol) in dry THF (30 mL) and NCS (269 mg, 2.01 mmol) in dry THF (30 mL) were allowed to react for 24 h at room temp. Flash chromatography with hexane/EtOAc (95:5) afforded 2-acetyl-5-chloropyrrole (**19**,[9e,18] 110 mg, 42%) as a colorless solid.

2-Acetylpyrrole (200 mg, 1.83 mmol) in dry THF (30 mL) and NCS (734 mg, 5.5 mmol) in dry THF (50 mL) were allowed to react for 72 h. Flash chromatography with hexane/EtOAc (95:5) afforded 2-acetyl-3,5-dichloropyrrole (**20**, 141 mg, 44%) as a colorless solid and 5-acetyl-2,3-dichloropyrrole (**21**,[18b] 125 mg, 39%) as a colorless solid.

2-Acetyl-3,5-dichloropyrrole (20): ^1H NMR (300 MHz, $CDCl_3$): δ = 10.09 (br. s, 1 H, NH), 6.07 (d, J = 3.0 Hz, 1 H, 3-H), 2.51 (s, 3 H, CH_3) ppm. ^{13}C NMR (75 MHz, $CDCl_3$): δ = 186.7 (CO), 127.6

(C-2), 122.5 (C5-Cl), 119.7 (C3-Cl), 110.4 (CH), 28.1 (CH_3) ppm. IR (neat): $\tilde{\nu}$ = 3218, 1643, 1446, 1400, 761 cm^{-1}. HRMS (EI): calcd. for $C_6H_5Cl_2NO$ 176.9749; found 176.9751.

5-Acetyl-2,3-dichloropyrrole (21): ^1H NMR (300 MHz, $CDCl_3$): δ = 10.81 (br. s, 1 H, NH), 6.76 (d, J = 2.7 Hz, 1 H, 4-H), 2.51 (s, 3 H, CH_3) ppm. ^{13}C NMR (75 MHz, $CDCl_3$): δ = 186.3 (CO), 128.0 (C-5), 120.5 (C2-Cl), 115.5 (CH), 110.5 (C3-Cl), 23.9 (CH_3) ppm. IR (neat): $\tilde{\nu}$ = 3218, 1643, 1447, 1399, 768 cm^{-1}. HRMS (EI): calcd. for $C_6H_5Cl_2NO$ 176.9749; found 176.9750.

5-Chloro-2-ethyl-4,4-difluoro-1,3,8-trimethyl-4-bora-3a,4a-diaza-*s*-indacene (12): 2-Acetyl-5-chloropyrrole (**19**,[9e,18] 91 mg, 0.63 mmol) in $CHCl_3$ (10 mL), $POCl_3$ (0.06 mL, 0.7 mmol), 3-ethyl-2,4-dimethylpyrrole (82 mg, 0.63 mmol) in $CHCl_3$ (10 mL), triethylamine (0.08 mL, 0.63 mmol), and $BF_3{\cdot}Et_2O$ (0.08 mL, 0.63 mmol) were allowed to react by the general procedure described above. Flash chromatography with hexane/$CHCl_3$ (5:5) afforded **12** (98 mg, 52%) as an orange solid; m.p. 171.2–171.7 °C. ^1H NMR (700 MHz, $CDCl_3$): δ = 6.90 (d, J = 4.2 Hz, 1 H, 7-H), 6.20 (d, J = 4.2 Hz, 1 H, 6-H), 2.51 (s, 3 H, CH_3), 2.44 (s, 3 H, CH_3), 2.35 (q, J = 7.7 Hz, 2 H, CH_2), 2.26 (s, 3 H, CH_3), 0.99 (t, J = 7.7 Hz, 3 H, CH_3CH_2) ppm. ^{13}C NMR (176 MHz, $CDCl_3$): δ = 161.1 (C), 140.7 (C), 138.6 (C), 135.7 (2 C), 134.0 (C), 133.1 (C), 122.8 (CH), 114.5 (CH), 17.1 (CH_2), 15.9 (CH_3), 14.5 (CH_3), 14.1 (CH_3), 13.1 (CH_3) ppm. IR (neat): $\tilde{\nu}$ = 1577, 1403, 1212, 1101, 771 cm^{-1}. HRMS (EI): calcd. for $C_{14}H_{16}BClF_2N_2$ 296.1060; found 296.1064.

5,7-Dichloro-2-ethyl-4,4-difluoro-1,3,8-trimethyl-4-bora-3a,4a-diaza-*s*-indacene (13): 2-Acetyl-3,5-dichloropyrrole (**20**, 90 mg, 0.50 mmol) in $CHCl_3$ (10 mL), $POCl_3$ (0.05 mL, 0.55 mmol), 3-ethyl-2,4-dimethylpyrrole (91 mg, 0.50 mmol) in $CHCl_3$ (10 mL), triethylamine (0.06 mL, 0.50 mmol), and $BF_3{\cdot}Et_2O$ (0.06 mL, 0.50 mmol) were allowed to react by the general procedure described above. Flash chromatography with hexane/EtOAc (98:2) afforded **13** (90 mg, 54%) as an orange solid; m.p. 193.1–193.6 °C. ^1H NMR (700 MHz, $CDCl_3$): δ = 6.21 (s, 1 H, 6-H), 2.72 (s, 3 H, CH_3), 2.51 (s, 3 H, CH_3), 2.36 (q, J = 7.7 Hz, 2 H, CH_2), 2.31 (s, 3 H, CH_3), 1.00 (t, J = 7.7 Hz, 3 H, CH_3CH_2) ppm. ^{13}C NMR (176 MHz, $CDCl_3$): δ = 162.2 (C), 141.7 (C), 139.8 (C), 137.0 (2 C), 135.0 (C), 133.2 (C), 127.2 (C), 126.4 (C), 115.6 (CH), 17.2 (CH_2), 16.3 (CH_3), 14.9 (CH_3), 14.4 (CH_3), 13.2 (CH_3) ppm. IR (neat): $\tilde{\nu}$ = 1568, 1417, 1375, 1194, 1084, 1031, 803 cm^{-1}. HRMS (EI): calcd. for $C_{14}H_{15}BCl_2F_2N_2$ 330.0668; found 330.0669.

5,6-Dichloro-2-ethyl-4,4-difluoro-1,3,8-trimethyl-4-bora-3a,4a-diaza-*s*-indacene (14): 5-Acetyl-2,3-dichloropyrrole (**21**, 90 mg, 0.50 mmol) in $CHCl_3$ (10 mL), $POCl_3$ (0.05 mL, 0.55 mmol), 3-ethyl-2,4-dimethylpyrrole (91 mg, 0.50 mmol) in $CHCl_3$ (10 mL), triethylamine (0.06 mL, 0.50 mmol) and $BF_3{\cdot}Et_2O$ (0.06 mL, 0.50 mmol) were allowed to react by the general procedure described above. Flash chromatography with hexane/EtOAc (95:5) afforded **14** (80 mg, 48%) as an orange solid; m.p. 187.3–187.8. ^1H NMR (700 MHz, $CDCl_3$): δ = 6.83 (s, 1 H, 7-H), 2.53 (s, 3 H, CH_3), 2.41 (s, 3 H, CH_3), 2.36 (q, J = 7.7 Hz, 2 H, CH_2), 2.28 (s, 3 H, CH_3), 1.00 (t, J = 7.7 Hz, 3 H, CH_3CH_2) ppm. ^{13}C NMR (176 MHz, $CDCl_3$): δ = 163.7 (C), 141.8 (C), 137.8 (C), 136.6 (2 C), 134.7 (C), 131.7 (C), 130.7 (C), 119.5 (CH), 116.2 (C), 17.1 (CH_2), 15.8 (CH_3), 14.4 (CH_3), 14.2 (CH_3), 13.3 (CH_3) ppm. IR (neat): $\tilde{\nu}$ = 1579, 1404, 1206, 1147, 1093, 1022, 801 cm^{-1}. HRMS (EI): calcd. for $C_{14}H_{15}BCl_2F_2N_2$ 330.0668; found 330.0670.

2-Chloro-4,4-difluoro-1,3,5,7,8-pentamethyl-4-bora-3a,4a-diaza-*s*-indacene (16): BODIPY **15** (60 mg, 0.23 mmol) in dry THF (15 mL) and NCS (37 mg, 0.28 mmol) in dry THF (5 mL) were allowed to react for 48 h. Flash chromatography with hexane/$CHCl_3$ (7:3) afforded **16** (50 mg, 73%) as an orange solid; m.p. 259.4–259.7 °C. ^1H NMR (700 MHz, $CDCl_3$): δ = 6.03 (s, 1 H, 6-H), 2.53 (s, 3 H, CH_3-C8), 2.46 (s, 6 H, CH_3-C3 and CH_3-C5), 2.36 (s, 3 H, CH_3-C7), 2.34 (s, 3 H, CH_3-C1) ppm. ^{13}C NMR (176 MHz, $CDCl_3$): δ = 156.0 (C-5), 148.3 (C-3), 142.8 (C-7), 141.7 (C-8), 134.1 (C-1), 132.7 (C-7a), 129.8 (C-8a), 122.1 (CH-6), 121.3 (C-Cl), 17.5 (CH_3-C7), 16.7 (CH_3-C8), 14.6 (CH_3-C5), 14.4 (CH_3-C1), 12.2 (CH_3-C3) ppm. IR (neat): $\tilde{\nu}$ = 1560, 1365, 1268, 1110 cm^{-1}. HRMS (ESI^+): calcd. for $[C_{14}H_{16}BClF_2N_2 + Na]^+$ 319.0961; found 319.0980.

2,6-Dichloro-4,4-difluoro-1,3,5,7,8-pentamethyl-4-bora-3a,4a-diaza-*s*-indacene (17): BODIPY **15** (50 mg, 0.19 mmol) in dry THF (15 mL) and NCS (76 mg, 0.57 mmol) in dry THF (10 mL) were allowed to react for 24 h. Flash chromatography with hexane/EtOAc (98:2) afforded **17** (42 mg, 67%) as an orange solid; m.p. 261.1–261.6 °C. ^1H NMR (700 MHz, $CDCl_3$): δ = 2.56 (s, 3 H, CH_3-C8), 2.48 (s, 6 H, CH_3-C3 and CH_3-C5), 2.35 (s, 3 H, CH_3-C1 and CH_3-C7) ppm. ^{13}C NMR (176 MHz, $CDCl_3$): δ = 150.7 (C-3 and C-5), 142.2 (C-8), 135.8 (C-1 and C-7), 130.4 (C-7a and C-8a), 122.4 (2 × C-Cl), 17.1 (CH_3-C8), 14.6 (CH_3-C1 and CH_3-C7), 12.3 (CH_3-C3 and CH_3-C5) ppm. IR (neat): $\tilde{\nu}$ = 1560, 1362, 1270, 1111 cm^{-1}. HRMS (EI): calcd. for $C_{14}H_{15}BCl_2F_2N_2$ 330.0668; found 330.0668.

Preparation of Solid Polymeric Samples: Solid matrices of PMMA incorporating some of the new fluorinated BDP dyes as true solutions were prepared essentially as described elsewhere.[4d] An appropriate amount of the dye was dissolved in pure MMA, which was polymerized to yield the materials named dye/PMMA. The solid samples were cast in a cylindrical shape, forming rods of 10 mm diameter and 10 mm length. A cut was made parallel to the axis of the cylinder to obtain a lateral flat surface of ca. 6 × 10 mm. This surface and the ends of the laser rods were prepared for lasing experiments with a grinding and polishing machine (Phoenix Beta 4000, Büehler) until optical-grade finishing. The planar grinding stage was carried out with a Texmet 1000 sand paper and 6 μm diamonds suspended in mineral oil as abrasive. The final polishing stage was carried out with a G-Tuch Microcloth and a cloth disk Mastertex with 1 μm diamonds in mineral oil.

Photophysical Properties: Solvents for laser and photophysical studies were of spectroscopic grade (Merck, Aldrich, or Sigma) and were used without purification; those used in synthetic work were purified by standard methods. Other reagents were from commercial sources, and used as received. The commercial laser dyes Pyrromethene 546 (Exciton) was used as received with a purity >99% (checked by spectroscopic and chromatographic methods). The monomer MMA (Merck) was successively washed with aqueous NaOH (5%) and water, dried with Na_2SO_4, and distilled under reduced pressure. Other reagents were from commercial sources and were used as received. The photophysical properties were determined in diluted solutions (around 2×10^{-6} M), prepared by adding the corresponding solvent (spectroscopic grade) to the residue from the appropriate amount of a concentrated stock solution in acetone, after vacuum evaporation of this solvent. UV/Vis absorption and fluorescence spectra were recorded with a Varian model CARY 4E spectrophotometer and a SPEX Fluorolog 3–22 spectrofluorimeter, respectively. Fluorescence quantum yields (ϕ) were determined by use of diluted dye solutions of suitable commercial BODIPYs (PM567 and PM650, ϕ = 0.84 and 0.10, respectively).[4a] Radiative decay curves were registered by the time-correlated single-photon-counting technique (Edinburgh Instruments, model FL920, fitted with a Hamamatsu C4878 microchannel plate detector), with picosecond time-resolution. Fluorescence emission was

monitored at the maximum emission wavelength after excitation at 470 nm and 530 nm with a diode laser (PicoQuant, model LDH470 and LDH530) with 150 ps FWHM pulses. The fluorescence lifetime (τ) was obtained after deconvolution of the instrumental response signal from the recorded decay curves by an iterative method. The goodness of the exponential fit was controlled by statistical parameters (chi-square, Durbin–Watson, and analysis of residuals). The radiative (k_{fl}) and nonradiative (k_{nr}) rate constants were calculated from the fluorescence quantum yield and lifetime; $k_{fl} = \phi/\tau$ and $k_{nr} = (1 - \phi)/\tau$. In the case of biexponential deconvolutions the amplitude-averaged lifetime – $<\tau>$ – was calculated as the sum of the products of each lifetime and their contibutions divided by 100. The corresponding rate constants were calculated from this average lifetime ($<k_{fl}>$ and $<k_{nr}>$).

Laser Experiments: Liquid solutions of dyes were placed in 1 cm optical path quartz cells carefully sealed to avoid solvent evaporation during experiments. The solutions of the newly synthesized dyes, as well as the solid samples, were transversely pumped at different wavelengths matching the maximum absorptions of the corresponding dyes: at 355 nm, with 5 mJ per pulse, 8 ns FWHM pulses from the third-harmonic of a Q-switched Nd:YAG laser (Spectron SL282G) and at 532 nm with 5.5 mJ, 6 ns FWHM pulses from a frequency-doubled Q-switched Nd:YAG laser (Monocrom OPL-10) at a repetition rate of 10 Hz. The exciting pulses were line-focused onto the cell, providing pump fluences on the active medium of 110 mJ cm^{-2}. The oscillation cavity (2 cm length) consisted of a 90% reflectivity aluminum mirror, with the lateral face of the cell as output coupler.

The photostabilities of the dyes were evaluated by irradiation of solutions in ethyl acetate (10 μL) under lasing conditions. Each solution was contained in a cylindrical Pyrex tube (1 cm height, 1 mm internal diameter) carefully sealed to avoid solvent evaporation during the experiments. Although the low optical quality of the capillary tube prevents laser emission from the dyes, information about photostabilities can be obtained by monitoring the decrease in laser-induced fluorescence intensity, excited transversally to the capillary tube, as a function of the number of pump pulses at 10 Hz repetition rate. The fluorescence emission was monitored perpendicular to the exciting beam, collected through an optical fiber, imaged onto the input slit of a monochromator (Acton Research corporation), and detected with a charge-coupled device (CCD, SpectruMM:GS128B). The fluorescence emission was recorded by feeding the signal to the boxcar (Stanford Research, model 250) for integration prior to digitization and processing by a computer. Each experience was repeated at least three times. The estimated error in the energy and photostability measurements was 10%.

Computational Details: All quantum mechanical calculations were performed with the aid of the Gaussian 03 package. Ground- and excited-state geometries were fully optimized by the Density Functional Theory (DFT) method (with use of B3LYP) and the Configuration Interaction Singles (CIS) ab initio method, respectively, with use of the double-valence basis set (6–31G). Absorption and fluorescence transitions were simulated by the time-dependent DFT (TD-DFT) method from the ground- and excited-state geometries, respectively.

X-ray Crystallographic Data: Crystals of BODIPYs **5**–**7** suitable for X-ray analysis were obtained by recrystallization from hexane. Crystal data were collected with an Agilent SuperNova Cu diffractometer and a CCD Atlas detector at 100 K.

CCDC-882023 (for **5**), -882022 (for **6**), and -882021 (for **7**) contain the supplementary crystallographic data for this paper. These data can be obtained free of charge from The Cambridge Crystallographic Data Centre via www.ccdc.cam.ac.uk/data_request/cif.

Supporting Information (see footnote on the first page of this article): copies of ^{1}H and ^{13}C NMR spectra of all new compounds, full photophysical and laser data for compounds **1**–**17** in different solvents, quantum mechanical simulations of their charge distributions and dipole moment orientations, and additional figures and tables mentioned in the article.

Acknowledgments

This work was supported by the Ministerio de Economia y Competitividad (MAT2010-20646-C04-01, MAT2010-20646-C04-02, MAT2010-20646-C04-03, MAT2010-20646-C04-04, and TRACE 2009-0144), the Comunidad de Madrid and the European Social Fund (S2009/PPQ-1634 "AVANCAT"), and the Gobierno Vasco (project number IT339-10). The SGI/IZO-SGIker UPV-EHU is gratefully thanked for allocation of computational resources. G. D. thanks Ministerio de Economía y Competitividad for an FPI fellowship.

[1] a) A. Loudet, K. Burgess, *Chem. Rev.* **2007**, *107*, 4891–4932; b) R. Ziessel, G. Ulrich, A. Harriman, *New J. Chem.* **2007**, *31*, 496–501; c) G. Ulrich, R. Ziessel, A. Harriman, *Angew. Chem.* **2008**, *120*, 1202; *Angew. Chem. Int. Ed.* **2008**, *47*, 1184–1201; d) F. L. Arbeloa, J. Bañuelos, V. Martinez, T. Arbeloa, I. L. Arbeloa, *Trends Phys. Chem.* **2008**, *13*, 101–122; e) A. C. Benniston, G. Copley, *Phys. Chem. Chem. Phys.* **2009**, *11*, 4124–4131; f) M. Benstead, G. H. Mehl, R. W. Boyle, *Tetrahedron* **2011**, *67*, 3573–3601; g) N. Boens, V. Leen, W. Dehaen, *Chem. Soc. Rev.* **2012**, *41*, 1130–1172.

[2] a) R. E. Pagano, C.-S. Chen, *Ann. N. Y. Acad. Sci.* **1998**, *845*, 152–160; b) R. E. Pagano, R. Watanabe, C. Wheatley, M. Dominguez, *Methods Enzymol.* **2000**, *312*, 523–534; c) Y. Gabe, Y. Urano, K. Kikuchi, H. Kojima, T. Nagano, *J. Am. Chem. Soc.* **2004**, *126*, 3357–3367; d) Z.-N. Sun, H.-L. Wang, F.-Q. Liu, Y. Chen, P. K. H. Tam, D. Yang, *Org. Lett.* **2009**, *11*, 1887–1890; e) A. Ojida, T. Sakamoto, M.-A. Inoue, S.-H. Fujishima, G. Lippens, I. Hamachi, *J. Am. Chem. Soc.* **2009**, *131*, 6543–6548; f) P. Didier, G. Ulrich, Y. Mely, R. Ziessel, *Org. Biomol. Chem.* **2009**, *7*, 3639–3642; g) X. Qian, Y. Xiao, Y. Xu, X. Guo, J. Qian, W. Zhu, *Chem. Commun.* **2010**, *46*, 6418–6436; h) J. O. Escobedo, O. Rusin, S. Lim, R. M. Strongin, *Curr. Opin. Chem. Biol.* **2010**, *14*, 64–70.

[3] a) A. Gorman, J. Killoran, C. O'Shea, T. Kenna, W. M. Gallagher, D. F. O'Shea, *J. Am. Chem. Soc.* **2004**, *126*, 10619–10631; b) S. O. McDonnell, M. J. Hall, L. T. Allen, A. Byrne, W. M. Gallagher, D. F. O'Shea, *J. Am. Chem. Soc.* **2005**, *127*, 16360–16361; c) T. Yogo, Y. Urano, Y. Ishitsuka, F. Maniwa, T. Nagano, *J. Am. Chem. Soc.* **2005**, *127*, 12162–12163; d) S. Atilgan, Z. Ekmekci, A. L. Dogan, D. Guc, E. U. Akkaya, *Chem. Commun.* **2006**, 4398–4400; e) S. Erbas, A. Gorgulu, M. Kocakusakogullari, E. U. Akkaya, *Chem. Commun.* **2009**, 4956–4958; f) S. Ozlem, E. U. Akkaya, *J. Am. Chem. Soc.* **2009**, *131*, 48–49; g) S. H. Lim, C. Thivierge, P. Nowak-Sliwinska, J. Han, H. van den Bergh, G. Wagnières, K. Burgess, H. B. Lee, *J. Med. Chem.* **2010**, *53*, 2865–2874; h) N. Adarsh, R. R. Avirah, D. Ramaiah, *Org. Lett.* **2010**, *12*, 5720–5723; i) H. He, P.-C. Lo, S.-L. Yeung, W.-P. Fong, D. K. P. Ng, *Chem. Commun.* **2011**, *47*, 4748–4750; j) H. He, P.-C. Lo, S.-L. Yeung, W.-P. Fong, D. K. P. Ng, *J. Med. Chem.* **2011**, *54*, 3097–3102; k) S. G. Awuah, J. Polreis, V. Biradar, Y. You, *Org. Lett.* **2011**, *13*, 3884–3887; l) Y. Cakmak, S. Kolemen, S. Duman, Y. Dede, Y. Dolen,

B. Kilic, Z. Kostereli, L. T. Yildirim, A. L. Dogan, D. Guc, E. U. Akkaya, *Angew. Chem.* **2011**, *123*, 12143; *Angew. Chem. Int. Ed.* **2011**, *50*, 11937–11941; m) Y. Chen, J. Zhao, L. Xie, H. Guo, Q. Li, *RSC Adv.* **2012**, *2*, 3942–3953; n) M. J. Ortiz, A. R. Agarrabeitia, G. Duran-Sampedro, J. Bañuelos Prieto, T. Arbeloa Lopez, W. A. Massad, H. A. Montejano, N. A. García, I. Lopez Arbeloa, *Tetrahedron* **2012**, *68*, 1153–1162; o) S. Duman, Y. Cakmak, S. Kolemen, E. U. Akkaya, Y. Dede, *J. Org. Chem.* **2012**, *77*, 4516–4527.

[4] a) F. Lopez Arbeloa, J. Bañuelos Prieto, V. Martinez, T. Arbeloa, I. Lopez Arbeloa, *Int. Rev. Phys. Chem.* **2005**, *24*, 339–374; b) O. Garcia, R. Sastre, D. del Agua, A. Costela, I. Garcia-Moreno, *Chem. Mater.* **2006**, *18*, 601–602; c) M. Liras, J. Bañuelos Prieto, M. Pintado-Sierra, F. Lopez Arbeloa, I. Garcia-Moreno, A. Costela, L. Infantes, R. Sastre, F. Amat-Guerri, *Org. Lett.* **2007**, *9*, 4183–4186; d) I. Garcia-Moreno, F. Amat-Guerri, M. Liras, A. Costela, L. Infantes, R. Sastre, F. Lopez Arbeloa, J. Bañuelos Prieto, I. Lopez Arbeloa, *Adv. Funct. Mater.* **2007**, *17*, 3088–3098; e) O. Garcia, R. Sastre, D. del Agua, A. Costela, I. Garcia-Moreno, F. Lopez Arbeloa, J. Bañuelos Prieto, I. Lopez Arbeloa, *J. Phys. Chem. C* **2007**, *111*, 1508–1516; f) O. Garcia, L. Garrido, R. Sastre, A. Costela, I. Garcia-Moreno, *Adv. Funct. Mater.* **2008**, *18*, 2017–2025; g) A. Costela, I. Garcia-Moreno, M. Pintado-Sierra, F. Amat-Guerri, M. Liras, R. Sastre, F. Lopez Arbeloa, J. Bañuelos Prieto, I. Lopez Arbeloa, *J. Photochem. Photobiol. A: Chem.* **2008**, *198*, 192–199; h) M. Alvarez, A. Costela, I. Garcia-Moreno, F. Amat-Guerri, M. Liras, R. Sastre, F. Lopez Arbeloa, J. Bañuelos Prieto, I. Lopez Arbeloa, *Photochem. Photobiol. Sci.* **2008**, *7*, 802–813; i) A. Costela, I. Garcia-Moreno, M. Pintado-Sierra, F. Amat-Guerri, R. Sastre, M. Liras, F. Lopez Arbeloa, J. Bañuelos Prieto, I. Lopez Arbeloa, *J. Phys. Chem. A* **2009**, *113*, 8118–8124; j) I. Garcia-Moreno, D. Zhang, A. Costela, V. Martin, R. Sastre, Y. Xiao, *J. Appl. Phys.* **2010**, *107*, 073105; k) M. J. Ortiz, I. Garcia-Moreno, A. R. Agarrabeitia, G. Duran-Sampedro, A. Costela, R. Sastre, F. Lopez Arbeloa, J. Bañuelos Prieto, I. Lopez Arbeloa, *Phys. Chem. Chem. Phys.* **2010**, *12*, 7804–7811; l) J. Bañuelos Prieto, A. R. Agarrabeitia, I. Garcia-Moreno, I. Lopez-Arbeloa, A. Costela, L. Infantes, M. E. Perez-Ojeda, M. Palacios-Cuesta, M. J. Ortiz, *Chem. Eur. J.* **2010**, *16*, 14094–14105; m) Y. Xiao, D. Zhang, X. Qian, A. Costela, I. Garcia-Moreno, V. Martin, M. E. Perez-Ojeda, J. Bañuelos, L. Gartzia, I. Lopez Arbeloa, *Chem. Commun.* **2011**, *47*, 11513–11515; n) D. Zhang, V. Martin, I. Garcia-Moreno, A. Costela, M. E. Perez-Ojeda, Y. Xiao, *Phys. Chem. Chem. Phys.* **2011**, *13*, 13026–13033; o) J. Bañuelos, V. Martin, C. F. A. Gomez-Duran, I. J. Arroyo Cordoba, E. Peña-Cabrera, I. Garcia-Moreno, A. Costela, M. E. Perez-Ojeda, T. Arbeloa, I. Lopez Arbeloa, *Chem. Eur. J.* **2011**, *17*, 7261–7270.

[5] L. Cerdan, A. Costela, I. Garcia-Moreno, O. Garcia, R. Sastre, *Opt. Express* **2010**, *18*, 10247–10256.

[6] L. Bonardi, H. Kanaan, F. Camerel, P. Jolinat, P. Retailleau, R. Ziessel, *Adv. Funct. Mater.* **2008**, *18*, 401–413.

[7] a) S. Hattori, K. Ohkubo, Y. Urano, H. Sunahara, T. Nagano, Y. Wada, N. V. Tkachenko, H. Lemmetyinen, S. Fukuzumi, *J. Phys. Chem. B* **2005**, *109*, 15368–15375; b) S. Erten-Ela, M. D. Yilmaz, B. Icli, Y. Dede, S. Icli, E. U. Akkaya, *Org. Lett.* **2008**, *10*, 3299–3302; c) T. Rousseau, A. Cravino, T. Bura, G. Ulrich, R. Ziessel, J. Roncali, *Chem. Commun.* **2009**, 1673–1675; d) T. Rousseau, A. Cravino, T. Bura, G. Ulrich, R. Ziessel, J. Roncali, *J. Mater. Chem.* **2009**, *19*, 2298–2300; e) D. Kumaresan, R. P. Thummel, T. Bura, G. Ulrich, R. Ziessel, *Chem. Eur. J.* **2009**, *15*, 6335–6339; f) T. Rousseau, A. Cravino, E. Ripaud, P. Leriche, S. Rihn, A. De Nicola, R. Ziessel, J. Roncali, *Chem. Commun.* **2010**, *46*, 5082–5084; g) C. Y. Lee, J. T. Hupp, *Langmuir* **2010**, *26*, 3760–3765; h) S. Kolemen, Y. Cakmak, S. Erten-Ela, Y. Altay, J. Brendel, M. Thelakkat, E. U. Akkaya, *Org. Lett.* **2010**, *12*, 3812–3815; i) B.-S. Kim, B. Ma, V. R. Donuru, H. Liu, J. M. J. Frechet, *Chem. Commun.* **2010**, *46*, 4148–4150; j) T. Kiliçoglu, Y. S. Ocak, *Microelectron. Eng.* **2011**, *88*, 150–154; k) T. Bura, N. Leclerc, S. Fall, P. Lévêque, T. Heiser, R. Ziessel, *Org. Lett.* **2011**, *13*, 6030–6033.

[8] a) M. Baruah, W. Qin, R. A. L. Vallée, D. Beljonne, T. Rohand, W. Dehaen, N. Boens, *Org. Lett.* **2005**, *7*, 4377–4380; b) T. Rohand, M. Baruah, W. Qin, N. Boens, W. Dehaen, *Chem. Commun.* **2006**, 266–268; c) T. Rohand, J. Lycoops, S. Smout, E. Braeken, M. Sliwa, M. Van der Auweraer, W. Dehaen, W. M. De Borggraeve, N. Boens, *Photochem. Photobiol. Sci.* **2007**, *6*, 1061–1066; d) W. Qin, T. Rohand, W. Dehaen, J. N. Clifford, K. Driesen, D. Beljonne, B. Van Averbeke, M. Van der Auweraer, N. Boens, *J. Phys. Chem. A* **2007**, *111*, 8588–8597; e) L. Li, B. Nguyen, K. Burgess, *Bioorg. Med. Chem. Lett.* **2008**, *18*, 3112–3116; f) O. Dilek, S. L. Bane, *Tetrahedron Lett.* **2008**, *49*, 1413–1416; g) O. Dilek, S. L. Bane, *Bioorg. Med. Chem. Lett.* **2009**, *19*, 6911–6913; h) E. Fron, E. Coutiño-Gonzalez, L. Pandey, M. Sliwa, M. Van der Auweraer, F. C. De Schryver, J. Thomas, Z. Dong, V. Leen, M. Smet, W. Dehaen, T. Vosch, *New J. Chem.* **2009**, *33*, 1490–1496; i) W. Qin, V. Leen, W. Dehaen, J. Cui, C. Xu, X. Tang, W. Liu, T. Rohand, D. Beljonne, B. Van Averbeke, J. N. Clifford, K. Driesen, K. Binnemans, M. Van der Auweraer, N. Boens, *J. Phys. Chem. C* **2009**, *113*, 11731–11740; j) L. Jiao, C. Yu, M. Liu, Y. Wu, K. Cong, T. Meng, Y. Wang, E. Hao, *J. Org. Chem.* **2010**, *75*, 6035–6038; k) D. W. Domaille, L. Zeng, C. J. Chang, *J. Am. Chem. Soc.* **2010**, *132*, 1194–1195; l) S. Yin, V. Leen, S. Van Snick, N. Boens, W. Dehaen, *Chem. Commun.* **2010**, *46*, 6329–6331; m) V. Leen, T. Leemans, N. Boens, W. Dehaen, *Eur. J. Org. Chem.* **2011**, *23*, 4386–4396; n) S. C. Dodani, S. C. Leary, P. A. Cobine, D. R. Winge, C. J. Chang, *J. Am. Chem. Soc.* **2011**, *133*, 8606–8616; o) L. Jiao, W. Pang, J. Zhou, Y. Wei, X. Mu, G. Bai, E. Hao, *J. Org. Chem.* **2011**, *76*, 9988–9996; p) V. Leen, D. Miscoria, S. Yin, A. Filarowski, J. M. Ngongo, M. Van der Auweraer, N. Boens, W. Dehaen, *J. Org. Chem.* **2011**, *76*, 8168–8176; q) X. Li, S. Huang, Y. Hu, *Org. Biomol. Chem.* **2012**, *10*, 2369–2372.

[9] a) C.-W. Wan, A. Burghart, J. Chen, F. Bergström, L. B.-A. Johansson, M. F. Wolford, T. G. Kim, M. R. Topp, R. M. Hochstrasser, K. Burgess, *Chem. Eur. J.* **2003**, *9*, 4430–4441; b) T. Rohand, W. Qin, N. Boens, W. Dehaen, *Eur. J. Org. Chem.* **2006**, 4658–4663; c) L. Bonardi, G. Ulrich, R. Ziessel, *Org. Lett.* **2008**, *10*, 2183–2186; d) D. Zhang, Y. Wen, Y. Xiao, G. Yu, Y. Liu, X. Qian, *Chem. Commun.* **2008**, 4777–4779; e) V. Leen, E. Braeken, K. Luckermans, C. Jackers, M. Van der Auweraer, N. Boens, W. Dehaen, *Chem. Commun.* **2009**, 4515–4517; f) Ö. A. Bozdemir, O. Büyükcakir, E. U. Akkaya, *Chem. Eur. J.* **2009**, *15*, 3830–3838; g) S. Rihn, P. Retailleau, N. Bugsaliewicz, A. De Nicola, R. Ziessel, *Tetrahedron Lett.* **2009**, *50*, 7008–7013; h) Y. Cakmak, E. U. Akkaya, *Org. Lett.* **2009**, *11*, 85–88; i) R. Guliyev, A. Coskun, E. U. Akkaya, *J. Am. Chem. Soc.* **2009**, *131*, 9007–9013; j) O. A. Bozdemir, Y. Cakmak, F. Sozmen, T. Ozdemir, A. Siemiarczuk, E. U. Akkaya, *Chem. Eur. J.* **2010**, *16*, 6346–6351; k) C. Thivierge, J. Han, R. M. Jenkins, K. Burgess, *J. Org. Chem.* **2011**, *76*, 5219–5228; l) T. K. Khan, M. Ravikanth, *Tetrahedron* **2011**, *67*, 5816–5824; m) S. Niu, G. Ulrich, P. Retailleau, R. Ziessel, *Tetrahedron Lett.* **2011**, *52*, 4848–4853; n) V. Lakshmi, M. J. Ravikanth, *Org. Chem.* **2011**, *76*, 8466–8471; o) S. Rihn, M. Erdem, A. De Nicola, P. Retailleau, R. Ziessel, *Org. Lett.* **2011**, *13*, 1916–1919; p) Y. Hayashi, S. Yamaguchi, W. Y. Cha, D. Kim, H. Shinokubo, *Org. Lett.* **2011**, *13*, 2992–2995; q) L. Fu, F.-L. Jiang, D. Fortin, P. D. Harvey, Y. Liu, *Chem. Commun.* **2011**, *47*, 5503–5505; r) D. T. Chase, B. S. Young, M. M. Haley, *J. Org. Chem.* **2011**, *76*, 4043–4051; s) T. Sakida, S. Yamaguchi, H. Shinokubo, *Angew. Chem.* **2011**, *123*, 2328; *Angew. Chem. Int. Ed.* **2011**, *50*, 2280–2283; t) T. K. Khan, R. R. S. Pissurlenkar, M. S. Shaikh, M. Ravikanth, *J. Organomet. Chem.* **2012**, *697*, 65–73.

[10] R. P. Sabatini, T. M. McCormick, T. Lazarides, K. C. Wilson, R. Eisenberg, D. W. McCamant, *J. Phys. Chem. Lett.* **2011**, *2*, 223–227.

[11] a) J. C. Koziar, D. O. Cowan, *Acc. Chem. Res.* **1978**, *11*, 334–341; b) K. N. Solovyov, E. A. Borisevich, *Phys. Usp.* **2005**, *48*, 231–253.
[12] a) M. Furst, H. Kallmann, F. H. Brown, *J. Chem. Phys.* **1957**, *26*, 1321–1332; b) B. Abrams, Z. Diwu, O. Guryev, S. Aleshkov, R. Hingorani, M. Edinger, R. Lee, J. Link, T. Dubrovsky, *Anal. Biochem.* **2009**, *386*, 262–269; c) X.-F. Zhang, I. Zhang, L. Liu, *Photochem. Photobiol.* **2010**, *86*, 492–498.
[13] a) K. Krumova, G. Cosa, *J. Am. Chem. Soc.* **2010**, *132*, 17560–17569; b) T.-I. Kim, S. Park, Y. Choi, Y. Kim, *Chem. Asian J.* **2011**, *6*, 1358–1361.
[14] J.-H. Ye, G. Wang, C. Huang, Z. Hu, W. Zhang, Y. Zhang, *Synthesis* **2012**, *44*, 104–110.
[15] a) L. Li, J. Han, B. Nguyen, K. Burgess, *J. Org. Chem.* **2008**, *73*, 1963–1970; b) V. Lakshmi, M. Ravikanth, *Dalton Trans.* **2012**, *41*, 5903–5911.
[16] A. Cui, X. Peng, J. Fan, X. Chen, Y. Wu, B. Guo, *J. Photochem. Photobiol. A: Chem.* **2007**, *186*, 85–92.
[17] B. J. Littler, M. A. Miller, C.-H. Hung, R. W. Wagner, D. F. O'Shea, P. D. Boyle, J. S. Lindsey, *J. Org. Chem.* **1999**, *64*, 1391–1396.
[18] a) C.-T. Ho, Q. Z. Gin, K. N. Lee, J. T. Carlin, *J. Agric. Food Chem.* **1982**, *30*, 362–364; b) R. A. Rane, V. N. Telvekar, *Bioorg. Med. Chem. Lett.* **2010**, *20*, 5681–5685.
[19] Q. Zheng, G. Xu, P. N. Prasad, *Chem. Eur. J.* **2008**, *14*, 5812–5819.
[20] M. A. H. Alamity, A. C. Benniston, G. Copley, K. J. Elliot, A. Harryman, B. Stewart, Y.-G. Zhi, *Chem. Mater.* **2008**, *20*, 4024–4032.
[21] F. Li, S. I. Yang, Y. Ciringh, J. Seth, C. H. Martin III, D. L. Singh, D. Kim, R. R. Birge, D. F. Bocian, D. Holten, J. S. Lindsey, *J. Am. Chem. Soc.* **1998**, *120*, 10001–10017.
[22] H. L. Kee, C. Kirmaier, L. Yu, P. Thamyongkit, W. J. Youngblood, M. E. Calder, L. Ramos, B. C. Noll, D. F. Bocian, W. R. Scheidt, R. R. Birge, J. S. Lindsey, D. Holten, *J. Phys. Chem. B* **2005**, *109*, 20433–20443.
[23] W. Qin, T. Rohand, M. Baruah, A. Stefan, M. Van der Auweraer, W. Dehaen, N. Boens, *Chem. Phys. Lett.* **2006**, *420*, 562–568.
[24] K. H. Drexhage, in: *Dye Laser* (Ed.: F. P. Schäfer), 3rd ed. Springer, Berlin, **1990**.
[25] L. Biczók, T. Bérces, F. Márta, *J. Phys. Chem.* **1993**, *97*, 8895–8899.
[26] P. O. Andersson, M. Bachilo, R.-L. Chen, T. Gillbro, *J. Phys. Chem.* **1995**, *99*, 16199–16209.
[27] P. Hartmann, M. J. C. Leiner, S. Draxler, M. E. Lippitsch, *Chem. Phys.* **1996**, *207*, 137–146.
[28] C. E. M. Carvalho, I. M. Brinn, A. V. Pinto, M. C. F. R. Pinto, *J. Photochem. Photobiol. A: Chem.* **2000**, *136*, 25–33.
[29] F. López Arbeloa, T. López Arbeloa, I. López Arbeloa, *J. Photochem. Photobiol. A: Chem.* **1999**, *121*, 177–182.
[30] F. López Arbeloa, J. Bañuelos, V. Martínez, T. Arbeloa, I. López Arbeloa, *ChemPhysChem* **2004**, *5*, 1762–1771.
[31] The dyes described in this work and their utilization as laser dyes are covered by Spanish Patent Application no. 201230486, filed on 30th March, **2012**.

Received: July 17, 2012
Published Online: October 4, 2012

